EXTENSIONAL RESPONSES TO TRANSTENSION IN THE MANUS BACKARC BASIN

A THESIS SUBMITTED TO THE GRADUATE DIVISION OF THE UNIVERSITY OF HAWAII IN PARTIAL FULFILLMENT OF THE REQUIREMENTS FOR THE DEGREE OF

MASTER OF SCIENCE

IN GEOLOGY AND GEOPHYSICS

AUGUST 1989

By
Robert Lawton Mallonee

Thesis Committee:

Brian Taylor, Chairman
Richard N. Hey
Frederick K. Duennebier

We certify that we have read this thesis and that, in our opinion, it is satisfactory in scope and quality as a thesis for the degree of Master of Science in Marine Geology and Geophysics.

THESIS COMMITEE

Brian Taylor

Chairman

Acknowledgements

The author would like to thank D. Hey, D. Naar, and J. Sinton for thought provoking discussions regarding this manuscript. The manuscript was significantly improved by thorough reviews by P. Cooper, F. Duennebier, D. Hey, M. Kleinrock, and D. Naar. This work was supported by National Science Foundation grant OCE-8511288.

Abstract

Extension in the Manus back-arc basin is occurring on a variety of spreading segments. Crust in the southeastern portion of the Manus Basin between the Weitin and Djaul transforms is being stretched giving rise to a number of en echelon sigmoidally shaped eruptive centers. Spreading is occurring in the southern part of the basin in a pair of overlapping rift graben. The magnetic signals over these two areas both have short wavelengths and normal polarity. The Manus Spreading Center is the fastest known backarc spreading center on Earth today with a spreading rate at its southwestern end of 118 mm/yr. Forward and inverse modelling of magnetic data constrains spreading rates along the length of the ridge and addresses whether a propagating rift, sphenochasm, microplate, or pull-apart model better explains the tectonics of this system. Although the magnetic evidence is not unequivocal, we prefer a model dominated by left-lateral shear and extension and incorporating a transtensional zone as a major tectonic element. SeaMARC II, seismicity, petrologic, and geochemical data support this preference.

Table of Contents

List of Figures

Introduction

The Bismarck Sea covers the backarc region of the New Britain island arc-trench system (Figure 1). The region is bisected by the northwest trending Willaumez-Manus Rise into the New Guinea and Manus Basins. The origin of the rise has yet to be resolved but it could have resulted from either a tectonic uplift that occurred as an active plate boundary was incised across the sea or from excess magmatism associated with hot spot activity [Johnson et al., 1979]. Connelly [1974] has designated the New Guinea and Manus Basins as two distinct tectonic provinces. He based this distinction on the lack of identifiable Brunhes magnetic anomalies and thicker sediments in the New Guinea Basin. Sediment thicknesses up to 2 km occur towards the margins of the sea. Connelly recognized an approximately 80 km wide, elongate sediment free area in the central Manus Basin, coincident with recent lava extrusion.

The Bismarck Sea is bordered on the north, east, and south by island arcs and on the southwest by the island arc terranes of the northern coastal ranges of Papua New Guinea [Pigram & Davies, 1987] (Figure 1). The island arc terranes have been episodically active since the mid-Cretaceous but most volcanic and tectonic activity occurred in Tertiary time [Connelly, 1975, 1976, Coleman & Packman, 1976, Kroenke, 1984]. Similar sequences of mostly Oligocene arc volcanics overlain and flanked by early to middle Miocene carbonates suggest that the Huon Peninsula and the islands

Figure 1. Plate boundaries, place names, locations of tectonic provinces, and structural elements in the Papua New Guinea region. Triangles on trench segments indicate direction of subduction; arrows indicate sense of motion on transform fault segments. The inset polygon outlines the survey area. Irregularly shaped black areas within the polygon are lava fields. All are coincident with extensional plate boundaries with the exception of the five smaller fields in the southwestern and western portions of the polygon which are thought to be outpourings from the base of the eastern scarp fo the Willaumez Rise. (modified from Cooper and Taylor, 1987)

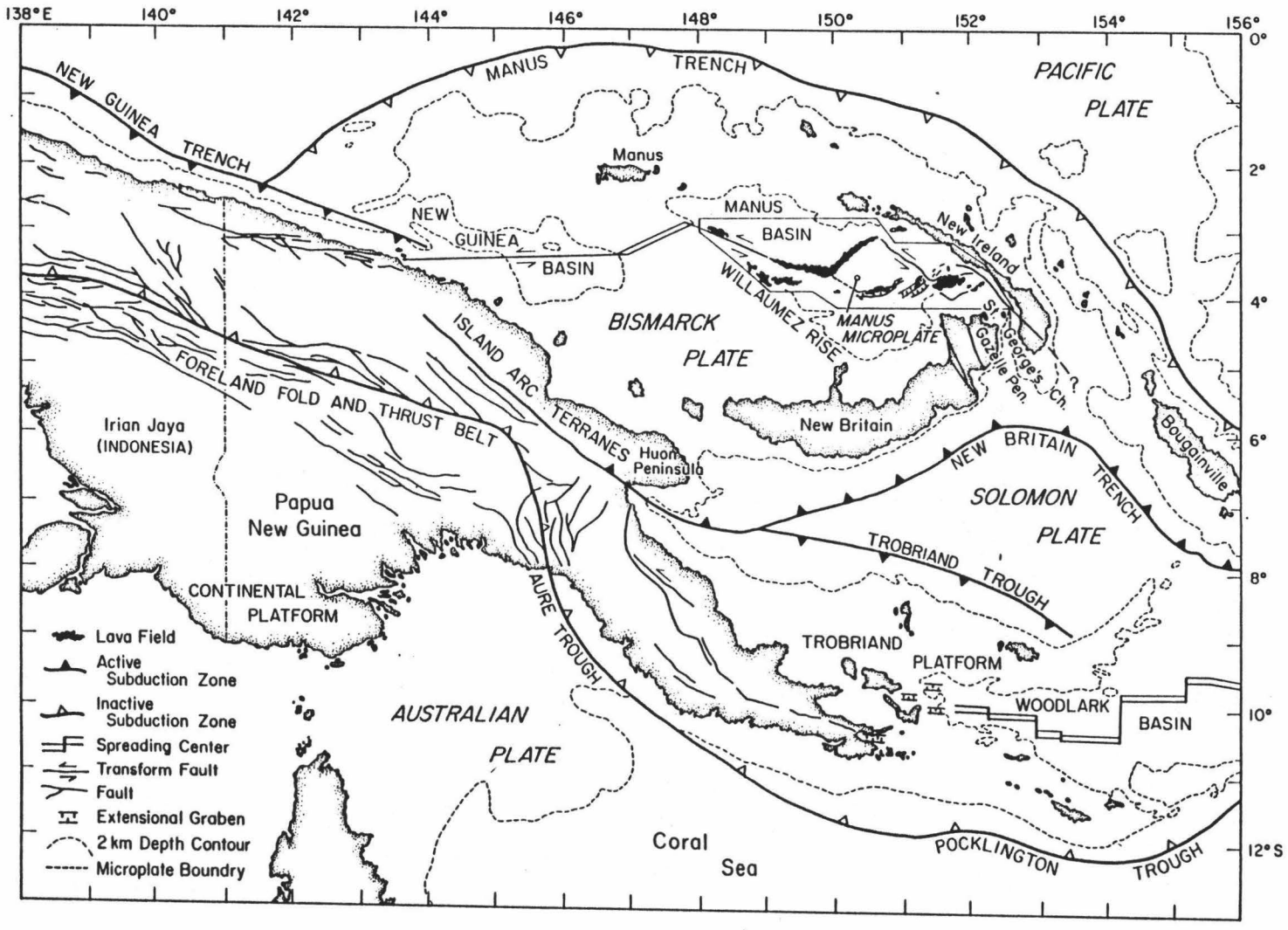
138°E
140°
142°
144°
146°
148°
150°
152°
154°
156°
0°
2°
4°
6°
8°
10°
12°S
NEW GUINEA TRENCH
MANUS TRENCH
PACIFIC PLATE
Manus
NEW GUINEA BASIN
MANUS BASIN
New Ireland
WILLAUMEZ RISE
MANUS MICROPLATE
St. George's Ch.
Gazelle Pen.
BISMARCK PLATE
FORELAND FOLD AND THRUST BELT
ISLAND ARC TERRANES
Huon Peninsula
New Britain
Irian Jaya (INDONESIA)
Papua New Guinea
NEW BRITAIN TRENCH
Bougainville
SOLOMON PLATE
TROBRIAND TROUGH
CONTINENTAL PLATFORM
AURE TROUGH
TROBRIAND PLATFORM
WOODLARK BASIN
AUSTRALIAN PLATE
Coral Sea
POCKLINGTON TROUGH
Lava Field
Active Subduction Zone
Inactive Subduction Zone
Spreading Center
Transform Fault
Fault
Extensional Graben
2 km Depth Contour
Microplate Boundry

bordering the Bismarck Sea and southeast through Bougainville to the Solomon Islands once formed a continuous mid-Tertiary island arc above a southwesterly subducting Pacific plate [Coleman & Packman, 1976, Kroenke, 1984]. On all the islands surrounding the Bismarck Sea the major fault trends are dominantly northwest, paralleling the Willaumez Rise. Manus, New Hanover, and New Ireland islands were uplifted in the Pliocene with New Ireland and New Hanover being tilted northeast away from the Manus Basin [Johnson et al., 1979]. Eocene and Oligocene arc volcanism on Manus, New Ireland and New Britain islands has intrusive cores which date well into the Miocene [Falvey & Pritchard, 1985].

Regional studies of earthquake seismicity and focal mechanisms of the western Pacific [Denham, 1969, Johnson and Molnar, 1972, and Curtis, 1973] identified a roughly E-W belt of seismicity defining a left-lateral strike-slip fault crossing the region at about 3° S. In a regional study of the Papua New Guinea–Solomon Islands, Ripper [1975] observed that the epicenters are too widely scattered to be a single transform fault. This band of shallow seismicity, known as the Bismarck Sea seismic lineation [Denham, 1969], delineates an active transtensional plate boundary stretching from St. George's Channel (4° 21'S, 152° 37.2'E) to the north coast of Papua New Guinea (3° 29.4'S, 143° 33'E) and detaches the Bismarck plate from the Pacific plate to the north (Figures 1 & 2). Based on focal mechanism and magnetic data, Taylor [1979] identified four linear segments to the seismic lineation, three of which have since been precisely located in the Manus Basin [Taylor et al., in prep.]

Figure 2. Shallow earthquakes and focal mechanisms which define the Bismarck Sea Seismic Lineation. Solid squares locate the ISC epicenters of earthquakes shallower than 50 km, with >4.7 m_b and recorded by fifteen or more stations during the years 1964 to 1983. Dots locate the epicenters of earthquakes shallower than 20 km, with <4.0 m_b and determined from a local OBS array deployed during the period from November 30 to December 27, 1983 [Eguchi et el., 1987] Focal mechanism solutions are for earthquakes during the years 1962 to 1981. Where possible, the focal mechanism solution is centered on the epicenter; in some cases the epicenter is indicated by an arrow drawn from the focal mechanism to the corresponding location. Compressional quadrants are stippled. Earthquake epicenters and focal mechanisms are not plotted below 5° S. Open triangles are inactive volcanoes. Solid triangles are active volcanoes. The inset polygon is the survey area for this study. The tapezium within the polygon outlines the approximate boundaries of the proposed Manus microplate. Earthquake data from Cooper, 1985, Dziewonski and Woodhouse, 1983, Pascal, 1979, Johnson and Molnar, 1972, Ripper, 1975, 1977, Taylor, 1979, and Weissel et al., 1982.


NEW IRELAND
NEW HANOVER
NEW BRITAIN
MANUS
PAPUA
NEW GUINEA
153°E
2°S
3°
4°
5°
152°
151°
150°
149°
148°
147°
146°
145°
144°

(Figure 1). Most recently, Eguchi et al. [1987] have deployed an ocean bottom seismometer array centered on the Willaumez transform. Focal mechanism solutions for this linear portion of the plate boundary are compatible with sinistral shear motion. However, Eguchi et al. also showed that the seismicity at the southeast end of the transform curves into the next seismic segment to the east (Figure 2).

Falvey and Pritchard [1985] have reported early findings from an ongoing paleomagnetic study in northeastern Papua New Guinea and on the islands surrounding the Bismarck Sea. Their data show that New Britain and the Huon Peninsula have acted as a single unit since the Pliocene and show the rotational effects of Manus Basin back-arc spreading. A plot of declination and inclination against time and reversal scale for 106 site means from New Britain and Huon Peninsula shows the following results: a declination which has varied between 30^{o} right declination and 45^{o} left declination during the past 45 Ma, while the inclination has decreased monotonically with age from approximately 30^{o} at 45 Ma. to about 06^{o} at present [Falvey & Pritchard, 1985, their figure 6]. From 4 Ma. to the present, the composite New Britain/Huon arc has rotated 15^{o} clockwise in response to backarc spreading in the Manus Basin with the Huon Peninsula having accreted to the New Guinea mainland along the Ramu-Markam suture.

The bulk of the marine data base for the Manus Basin comes from two systematic marine geophysical surveys of that area: a 1970 Australian Bureau of Mineral Resources (BMR5A) cruise and a

1985 CCOP/SOPAC-Hawaii Institute of Geophysics (MW8517) survey (Figure 3). Additional data are available from other geophysical cruises through the area conducted by Hawaii Institute of Geophysics (MH70042202/03), Lamont-Doherty Geological Observatory (V3313), and University of Tokyo (KH6705 & KH7104).

During the Bureau of Mineral Resources cruise bathymetric, magnetic, gravity, and seismic reflection data were gathered along north-south tracklines. The survey covered the entire Bismarck Sea with 30-40 km spacing between tracklines. Based on these data Connelly [1975, 1976] concluded that the Manus Basin has an axial sediment-free area of normally magnetized material. Since New Hanover forms part of the northern boundary to the sediment-free area he postulated asymmetrical spreading to the south with a spreading rate of 80 mm/yr full rate over the past 2.5 my. Connelly assumed the site of spreading to be a 10 km wide non-magnetic plug which he deduced to be near the center of the normally magnetized material. However, his gravity modelling did not demonstrate the presence of low density material under the conjectured spreading axis location. The magnetic anomalies near the seismic belt showed a preferred easterly trend, although, as Hamilton [1979] points out, the gridding for the computer contoured magnetic anomaly map strongly biased the contouring toward east-west anomalies. Thus discrimination of short anomaly lineations trending north-northeast and separated by west-northwest transforms was impossible.

Figure 3. Tracklines for surveys conducted in the eastern and central Manus Basin, Bismarck Sea. Arrows on the MW8517 tracklines indicate the direction in which the trackline was sailed. Numbers on the MW8517 tracklines indicate trackline and profile numbers referred to in the text and figures 7 and 10c.

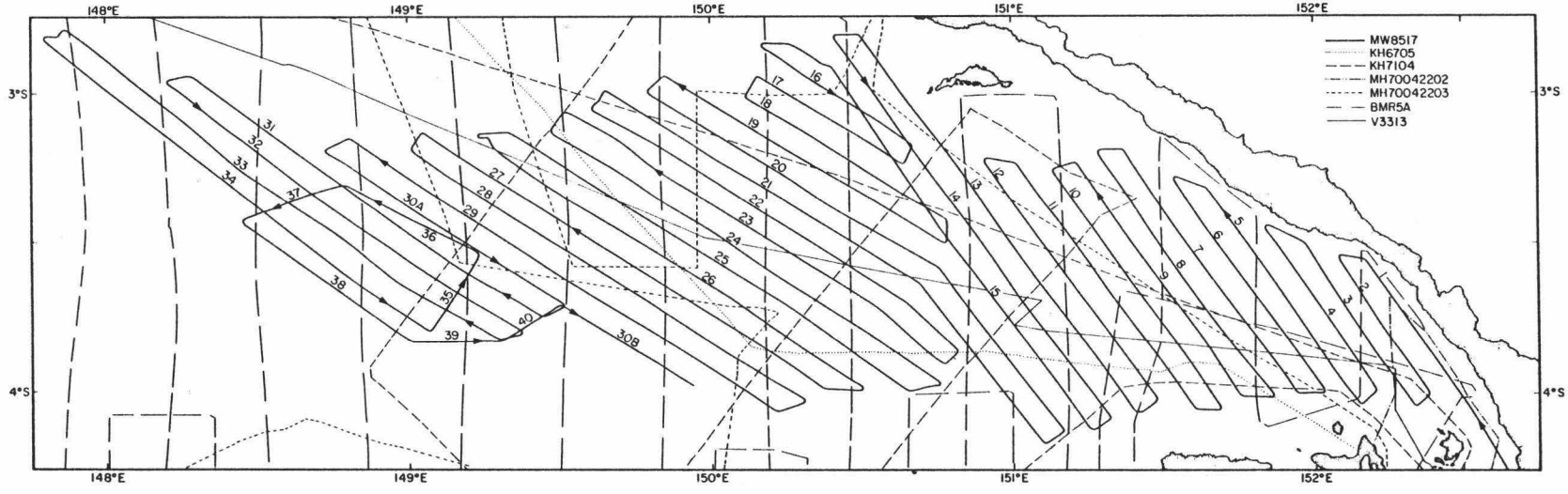
148°E
149°E
150°E
151°E
152°E
3°S
4°S
MW8517
KH6705
KH7104
MH70042202
MH70042203
BMR5A
V3313

Based on forward modelling of magnetics data from the R/V Vema trackline (V3313, Figure 3) traversing the Manus Basin on an azimuth of 110^{o} to 115^{o}, Taylor [1979] postulated asymmetric spreading to the north for the Manus Spreading Center. He identified magnetic lineations out to Anomaly 2' and proposed a full spreading rate over the last 3.5 my of 132 mm/yr: 74 and 58 mm/yr on the northern and southern limbs , respectively.

In this study the magnetic anomaly data from the 1985 Moana Wave survey are presented and interpreted . The applicability of a sphenochasm versus a propagating rift model for the central spreading ridge and a microplate versus a diffuse deformation model for the basin will be explored. We present magnetic anomaly profiles along tracklines (Figure 4), magnetic contour (Figure 5) and magnetization (Figure 6) maps for the basin and forward models (Figure 7) for the central spreading segment to investigate the relationship between the sinistral shear motion which dominates the Pacific/Bismarck plate boundary and the tectonic structures found in the basin. The possible physical constraints affecting the spreading styles active in the basin are discussed, and the nature of the central spreading ridge is considered.

Figure 4 Magnetic anomaly profiles over the Manus Basin using ship tracks as baselines (zero anomaly). Anomaly profiles were obtained by subtracting the 1975 International Geomagnetic Reference Field adjusted to 1985 from the measured magnetic total field values. Solid line segments locate tectonic features identified in Figure 8b (p. 22). Dashed line segments locate the magnetic anomaly resulting from the Emperor reversed event.

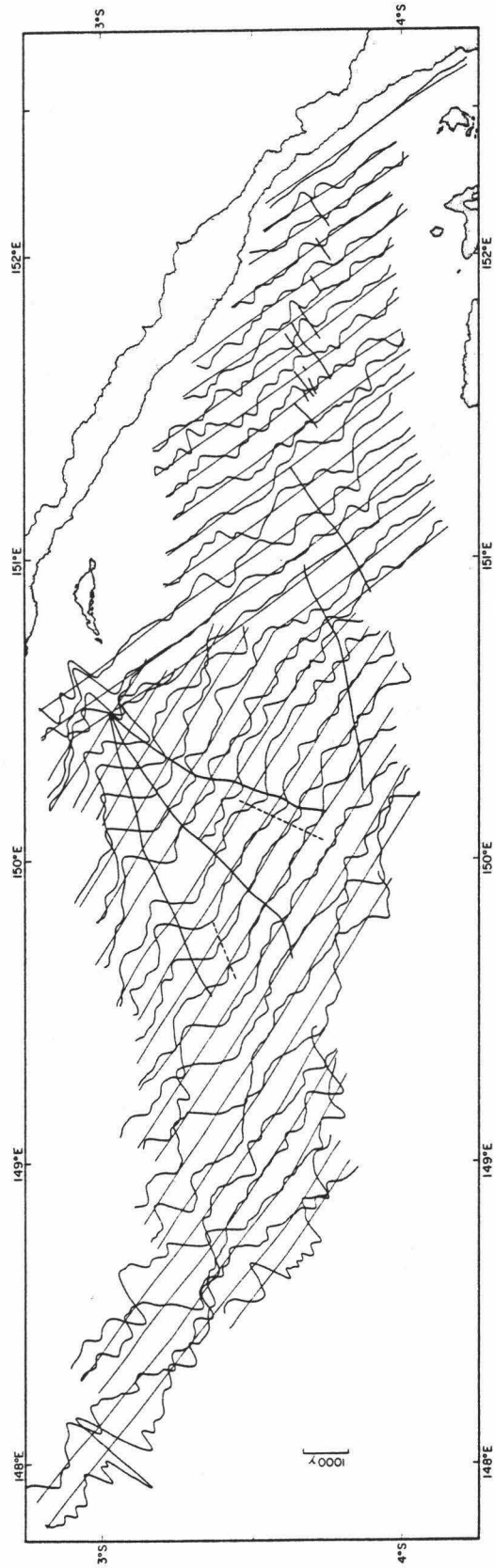
3°S
4°S
152°E
151°E
150°E
149°E
148°E
1000γ

Figure 5 Hand contoured magnetics for the survey area. Contour interval is 100 nT. The warm colors are positively i.e. reversely polarized crust and the cool colors are the negatively i.e. normally polarized crust.

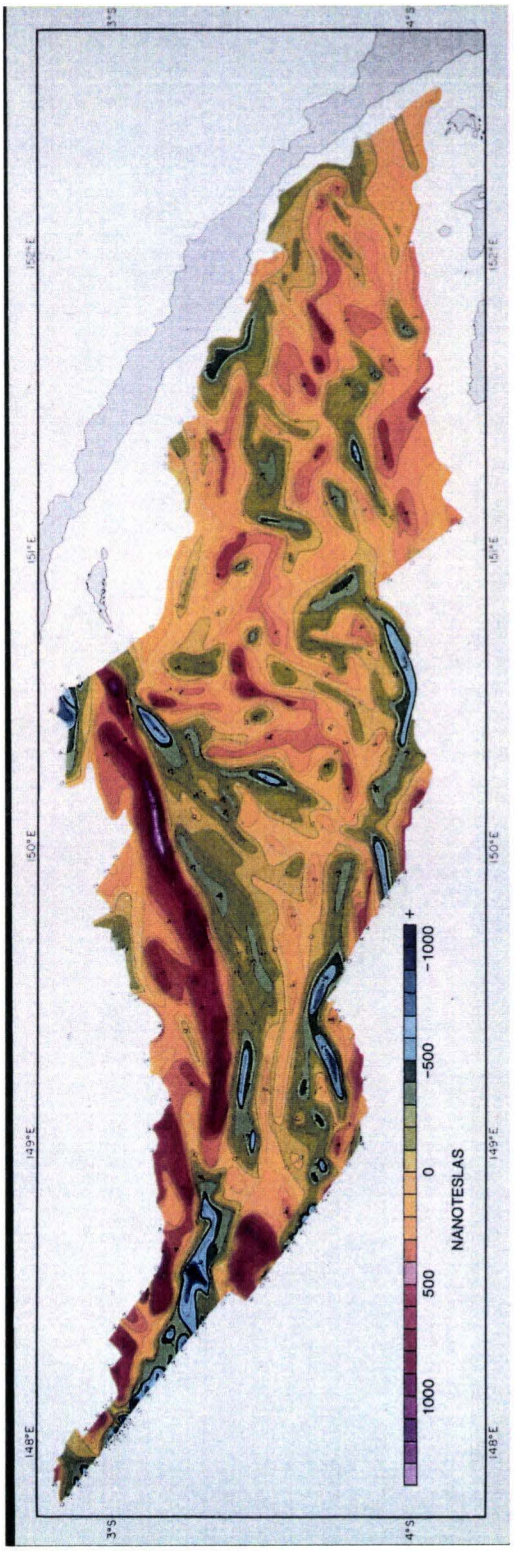
148°E
149°E
150°E
151°E
152°E
3°S
4°S
+
1000
500
0
−500
−1000
NANOTESLAS

Figure 6. Magnetization profiles for the eastern Manus Basin. The magnetization was determined from magnetic anomaly profiles projected perpendicular to the extensional plate boundary segments which they cross, the resulting magnetization then being displayed along the unprojected track segments. Profiles east of 151°E longitude are projected at 145°. Northwestern portions of profiles crossing the Manus Spreading Center between 150° 30'E and 150°E are projected at 149°. Portions of profiles south of the dashed line are projected at 165°. Portions of profiles north and west of the dashed lines are projected at 135°. The ship tracks are used as baselines (zero magnetization). In some cases ship tracks with nonlinear portions have been represented by straight segments that only approximate the true trackline.

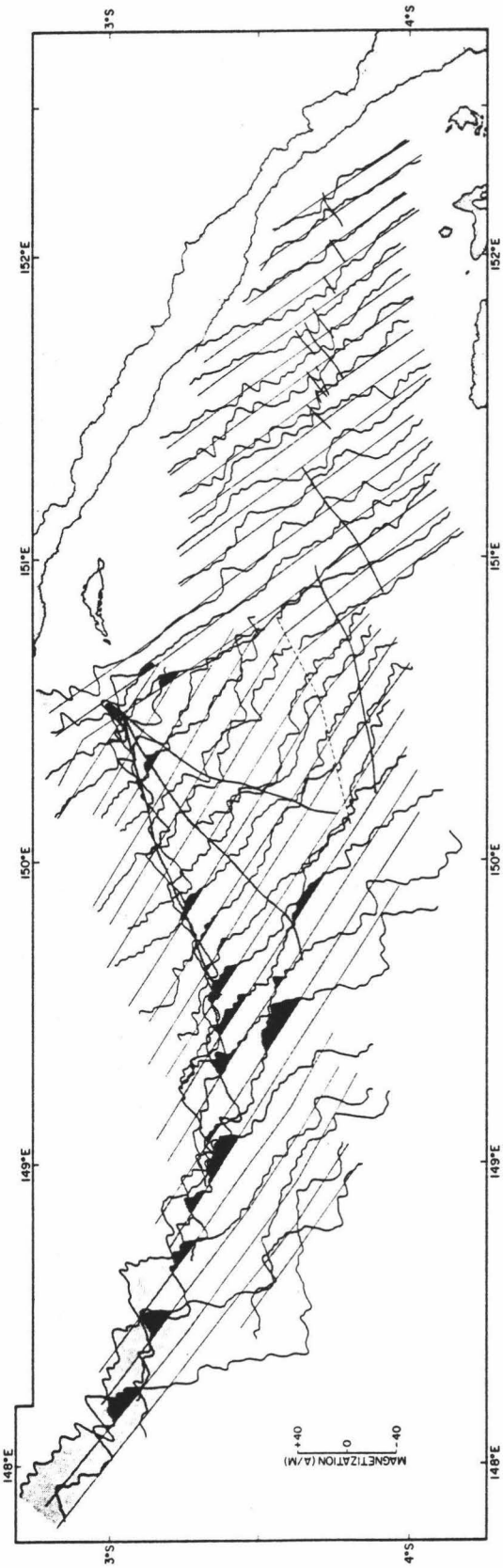
3°S
4°S
152°E
151°E
150°E
149°E
148°E
MAGNETIZATION (A/M)
+40
0
-40

Figure 7. Magnetic anomaly data and synthetic models for tracklines 17-26 shown in figure 3 arranged from northeast to southwest. The top profile represents the data (nT), the middle profile is the forward model (solid line portions of the profile are the models that fit the data; dashed lines are portions of the model profile which do not fit the data), and the lower profile is the associated reversal block model superimposed on bathymetry (m). Some parameters are common to all model profiles. These include: effective susceptibility (0.032), thickness of magnetic layer (1.0 km), and spacing between computed points (0.25 km), and intensity (1.5 A/M). The numbers in the upper righthand corner of each data/model pair box matches the trackline numbers of figure 3. Full spreading rates (sr) and asymmetries (a) used to generate each model are indicated for all data/model pairs. Positive asymmetry means left side spreads faster and negative asymmetry means right side spreads faster.

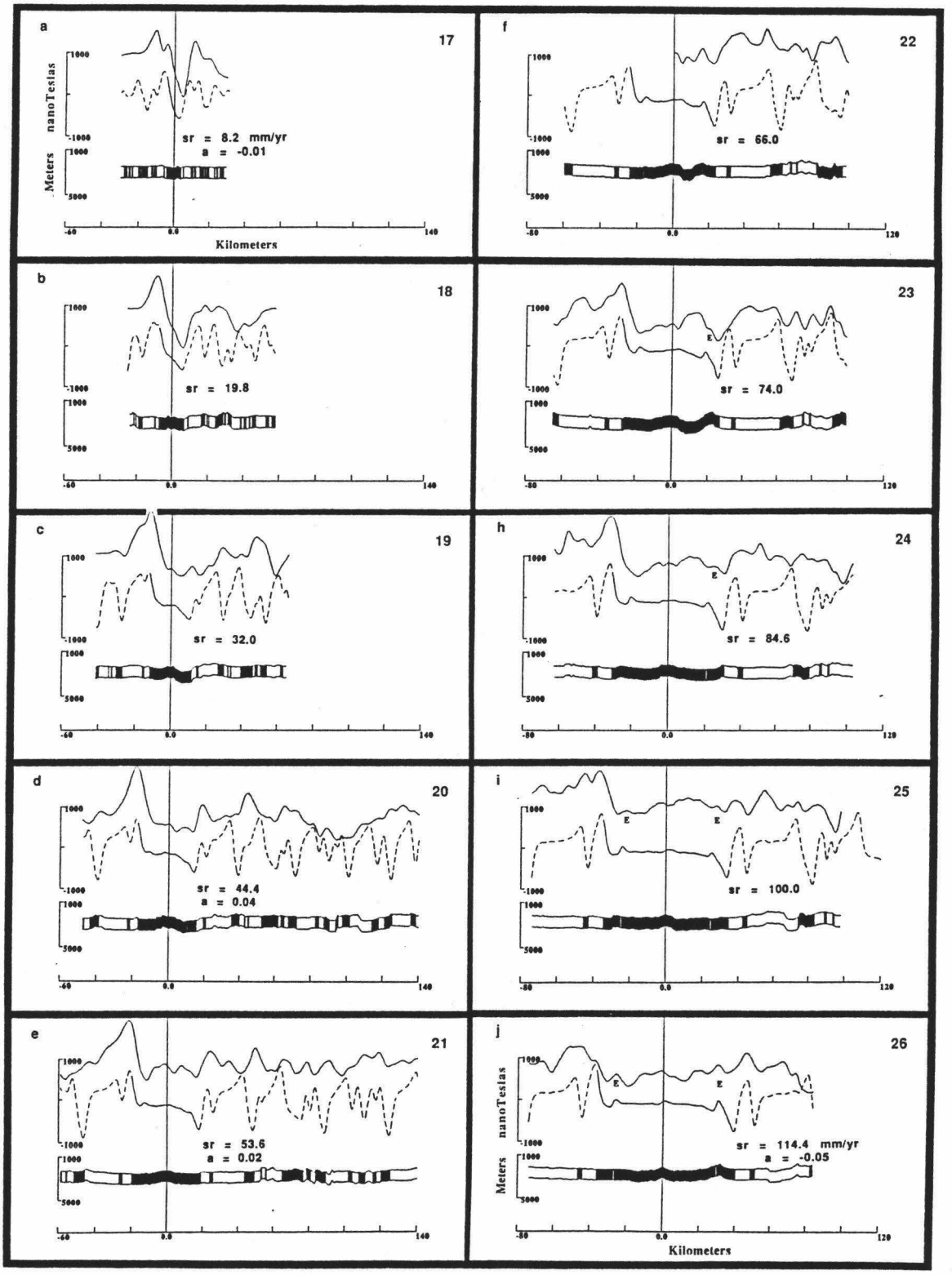
a
17
nanoTeslas
Meters
sr = 8.2 mm/yr
a = -0.01
Kilometers
b
18
sr = 19.8
c
19
sr = 32.0
d
20
sr = 44.4
a = 0.04
e
21
sr = 53.6
a = 0.02
f
22
sr = 66.0
23
sr = 74.0
h
24
sr = 84.6
i
25
sr = 100.0
j
26
sr = 114.4 mm/yr
a = -0.05
Kilometers

Tectonic Setting

New Data

In December 1985 the R/V Moana Wave acquired SeaMARC II bathymetry and sidescan, 3.5 kHz bathymetric, magnetic, and gravity data along 5300 km of predominately northwest-southeast track lines in the Manus Basin (Figure 3). The SeaMARC II side scan coverage totals 41,000 km^2. Trackline spacing varies between 8 and 8.5 km with the survey concentrating on the main structural features in and bounding the central and eastern Manus Basin. The trackline orientation is approximately perpendicular to the extensional plate boundary segments and subparallel to the transform boundary segments in the basin. The spacing between tracklines is much closer than that for the previously mentioned Bureau of Mineral Resources survey. This provides an extensive data base for interpretation of the tectonics in the Manus Basin.

While this paper relies on the sidescan data for supporting evidence, it concentrates on interpretation of the magnetic data. A paper focusing on the SeaMARC II data is forthcoming [Taylor et al., in prep.] but an overview of the resulting tectonic interpretation will be given here to put the magnetics in context.

Figure 8. a. SeaMARC II mosaic of survey area. b. Line drawing and tectonic interpretation of the SeaMARC II mosaic. WIT, Willaumez transform; ETZ, "extensional transform zone"; RJB, ridge jump boundary; MSC; Manus Spreading Center; DJT, Djaul transform; SWB, southwestern microplate boundary; SR, southern rifts; SER, southeastern en echelon ridges; WET, Weitin transform. Stippled areas are lava fields. (figure 8a after Taylor, unpub. figure)

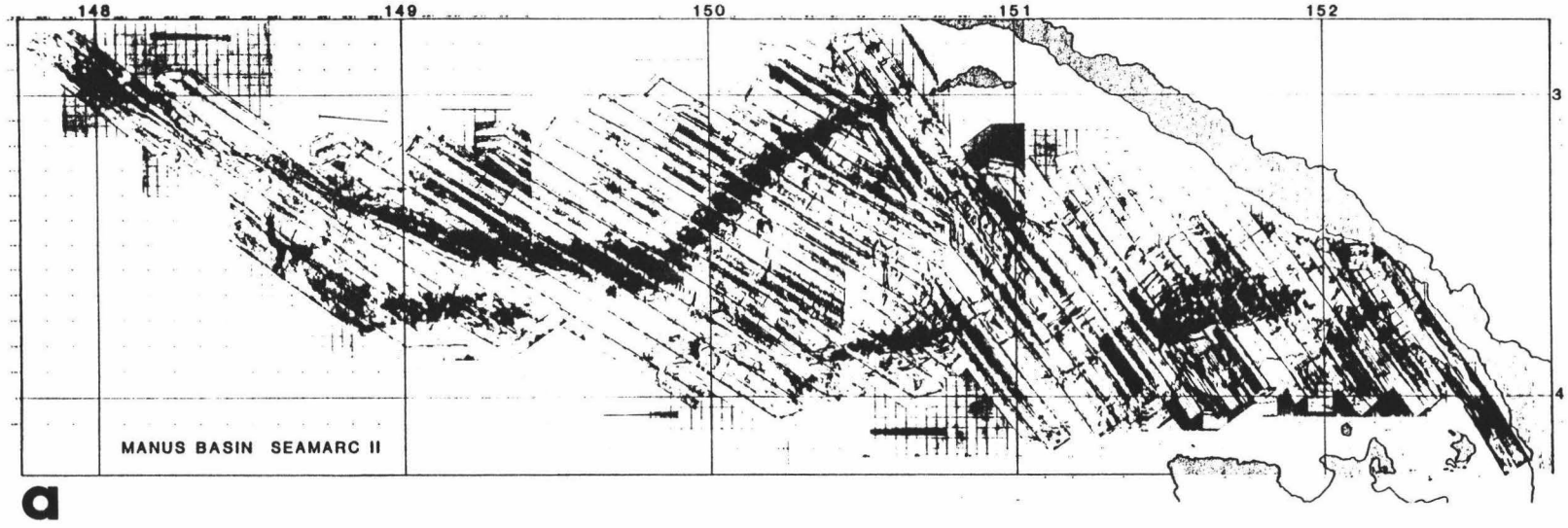
148
149
150
151
152
3
4
MANUS BASIN SEAMARC II

a

b

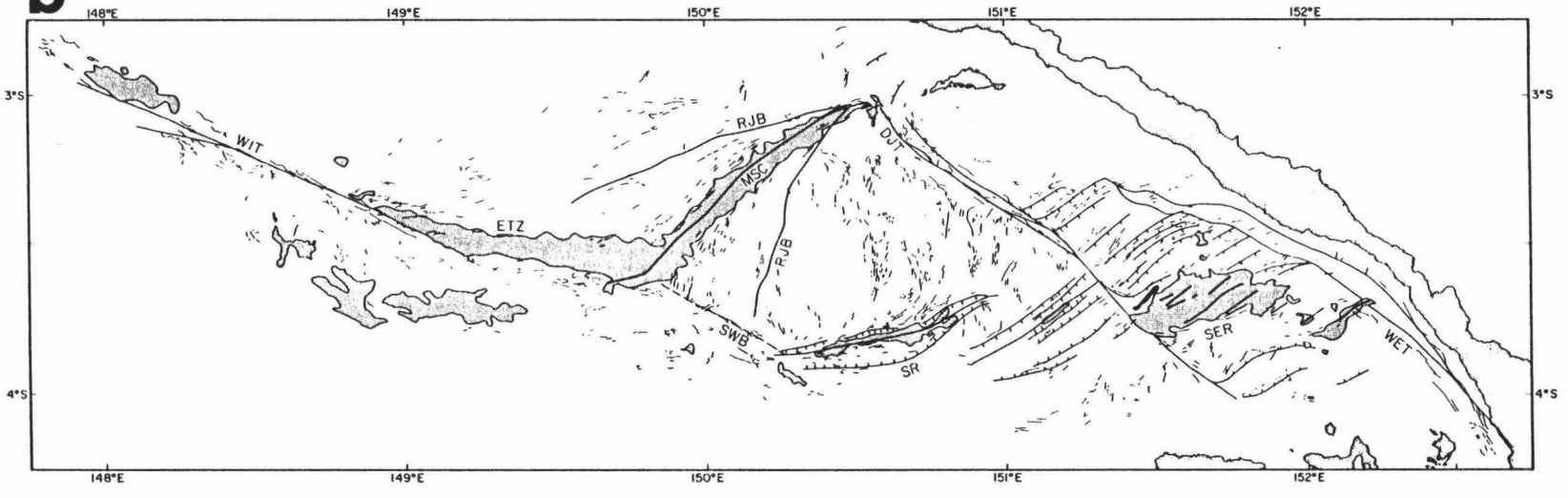
148°E
149°E
150°E
151°E
152°E
3°S
4°S
WIT
ETZ
RJB
MSC
DUT
RJB
SWB
SR
SER
WET

Manus Basin

The tectonic interpretation for the eastern Manus Basin can be seen in figure 8b. It is evident that the basin can be divided into provinces bounded by sinistral strike-slip faults. The south coast of New Ireland, which parallels the northwestern extension of the Weitin fault, acts as the eastern basinal margin (Figure 8). A series of volcanically active, east-northeast trending en echelon spreading segments lie within a pull-apart zone between the Weitin and Djaul transforms. Along strike to the southeast of the Djaul Transform, a series of high-angle faults, termed by Lindley [1988] the Baining Mountain Horst and Graben Zone, cut north-northwest across the Gazelle Peninsula (Figures 1 & 2). To the southwest of the Djaul transform there is a 12,000 km^2 rhomb-shaped area enclosed by four active boundaries which Taylor et al. [1987] named the Manus microplate. We will argue in the discussion section that a microplate model is not a viable paradigm for this area. Rather, we will argue for a "transtensional zone" in which extension is being accommodated along its northwestern boundary by localized spreading and in its interior by distributed stretching. The Djaul fault forms the NE border of the "transtensional zone". The southern edge of the "transtensional zone" is composed of a pair of overlapping rift grabens with axial lava flows. These grabens overlap by approximately 17 km with a separation of about 12 km. The southwestern boundary of the "transtensional zone" is poorly defined and is located along the edge of a bathymetric high (Figure

Figure 9. Color contoured bathymetry for the Manus Basin. Hot colors are shoal areas. Cool colors are deeps. (modified from Taylor, unpub. figure)


NEW IRELAND
3°
4°
152°
150°
149°
148°
METRES
200
600
1000
2000
3000

9) which may be a transform fault [Taylor et al., 1987]. Evidence for its existence comes from the contoured magnetics for the basin (Figure 5) where a stripe of normally magnetized crust has the same strike and occupies the same location as the proposed bounding transform fault (3° 50'S, 150° 05'E). The 110 km long sigmoidally shaped Manus Spreading Center makes up the northwestern perimeter of the alleged microplate (Figure 8). Between the fast slipping Willaumez transform and the southwestern end of the Manus Spreading Center lies the 90 km-long "extensional transform zone" [Taylor, et al., 1986]. The "extensional transform zone" is characterized by volcanism and extension as well as left lateral strike-slip motion. It is comprised of overlapping, right-stepping, en echelon spreading segments trending N72°E [Taylor et al., 1986; Eguchi, et al., 1987] that are cut by a Riedel shear (trend 105°) synthetic to the Willaumez transform. The geometry of the structural elements of the "extensional transform zone" fits that of a second order strain ellipse to the Willaumez transform [Taylor, et al., 1986]. This means that the orientation of the structural elements making up the "extensional transform zone" matches the orientation of any secondary structural elements (e.g. Riedel shears and tension fractures) associated with the primary structure, the Willaumez transform. The Willaumez fault marks the eastern edge of the Willaumez Rise that bounds the Manus Basin to the west (Figures 1 & 8).

Six of the lava fields seen on the SeaMARC II mosaic in figure 8a are associated with plate and microplate boundaries. Five of these fields are related to segments of the extensional boundaries. The sixth field (3°S, 148° 05'E) and another located near 3° 36'S, 148° 58'E, are thought to be cogeneric with Willaumez Rise magmatism [Sinton, pers. comm., 1988]. It is thought that the magma has used the fault structure at the base of the eastern scarp of the Willaumez Rise as a conduit to the surface. However, since neither of these latter fields have been sampled petrologically this is speculative.

Manus Spreading Center

The Manus Spreading Center is the main spreading axis present in the Manus Basin. It trends northeast-southwest and is bounded at its northeastern extremity by the Djaul transform and on its southwestern end by the "extensional transform zone" (Figure 8). For the easternmost 40 km of its length the spreading axis occupies a graben that has a maximum depth of over 2600 m and is approximately 2-3 km wide (Figure 9 & 10a). This morphological expression corresponds to the region of small crustal generation, determined by our forward modelling to range between 0 and 33 km. It could be either a result of slow spreading rate or rift propagation (magmatic supply not fully matching the spreading rate). However, beyond 3° 08.2'S, 150° 19.4'E the crustal generation is fast enough and the magmatic supply is robust enough so that an axial volcano

Figure 10 a. contoured bathymetry for the Manus Spreading Center. b. relief along the Manus spreading center showing the location of the deviation from axial linearity (Deval). c. crustal generation (km/my) vs. distance along the Manus Spreading Center (km). Open error bars indicate differring assumptions used in determining crustal generation values. See text for explanation. (figures 10a and 10b modified from Liu, 1989)

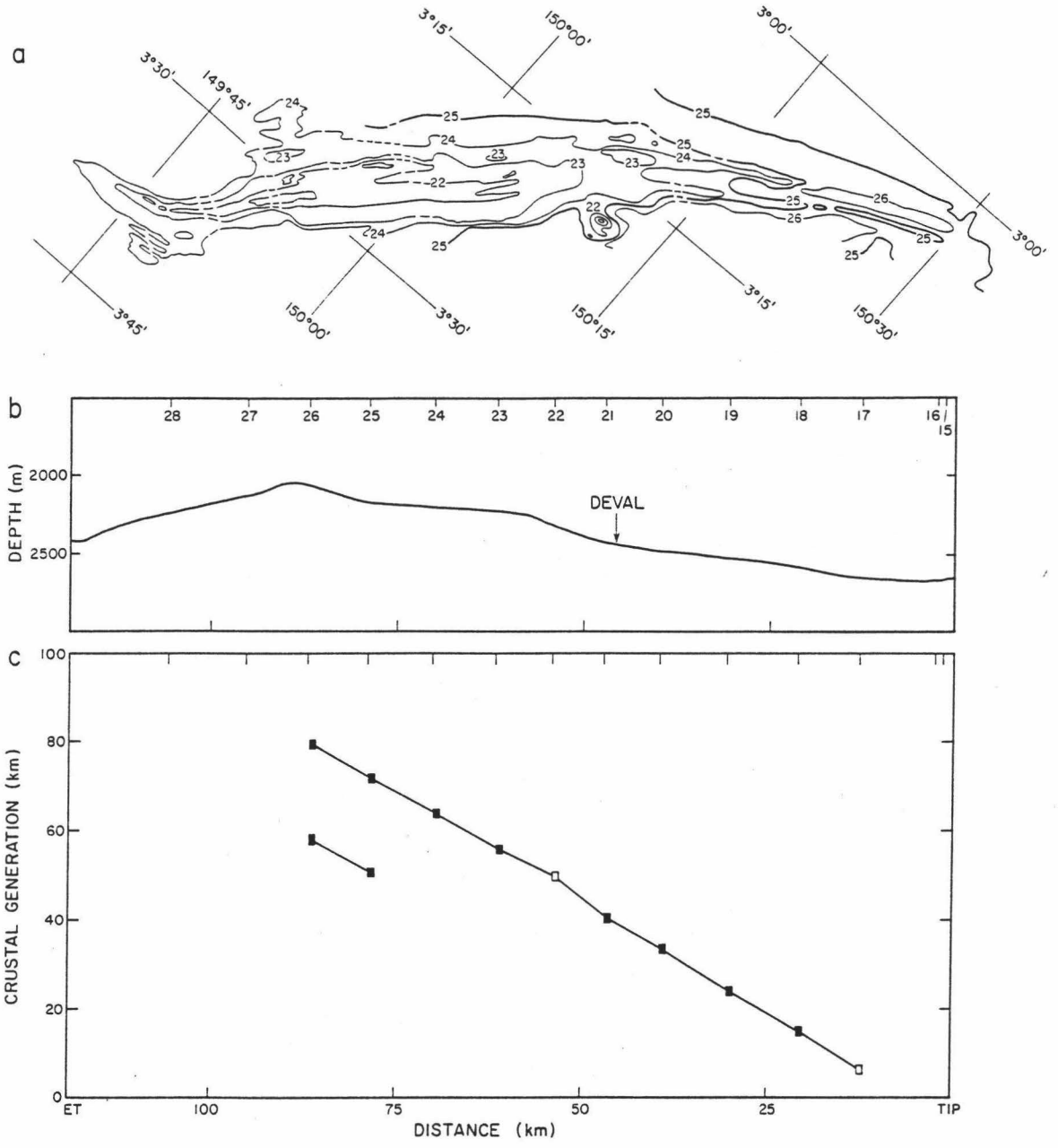
a
3°15'
150°00'
3°00'
3°30'
149°45'
3°45'
150°00'
3°30'
150°15'
3°15'
150°30'
3°00'
b
28 27 26 25 24 23 22 21 20 19 18 17 16/15
DEPTH (m)
2000
2500
DEVAL
c
CRUSTAL GENERATION (km)
100
80
60
40
20
0
ET
100
75
50
25
TIP
DISTANCE (km)

Figure 11 Seismic reflection profiles across the Manus Spreading Center . The rift axis is located by the dashed line. Ridge jump boundaries shown by solid lines. Numbers to the left of the profiles correspond to trackline numbers used in figure 3. (modified from Taylor, unpublished figure)

SPREADING CENTER

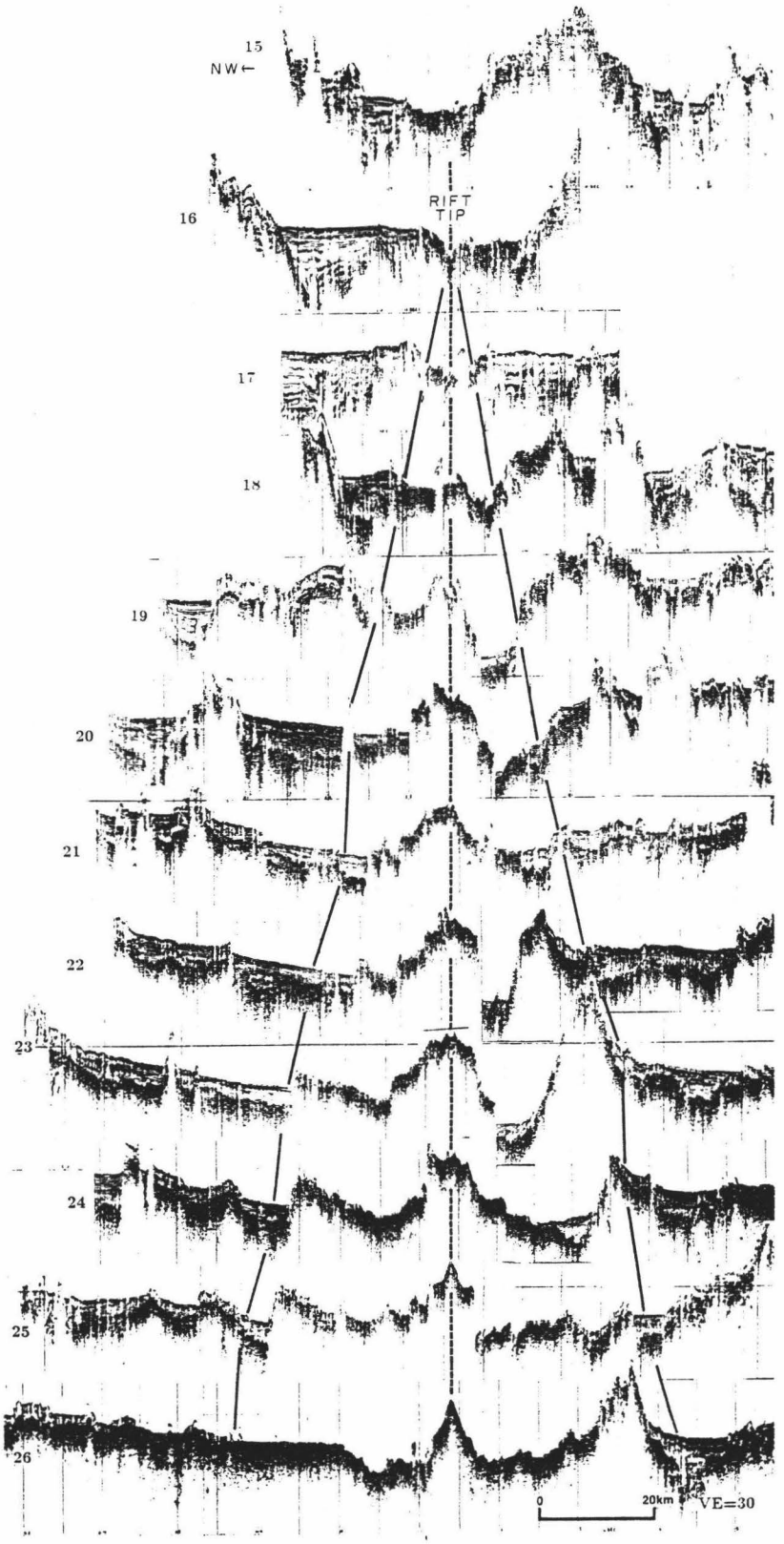

begins to emerge (profile 18, Figure 11). It is near here that Both et al., [1986] photographed active hydrothermal vents (near 3° 09.7'S, 150° 16.8'E) and Craig and Poreda, [1987] sampled water (3° 10.8'S, 150° 15.1'E) that had a large methane anomaly. They attributed this anomaly to the hydrothermal activity. Helium isotope ratios for basalts dredged at this site average R/R_A=11.2 (mid-ocean ridge basalt ratios are about 8.0) indicating a plume type mantle as one of the sources [Craig and Poreda, 1987]. The axis continues to shoal until at approximately 92 km (3° 31.5'S, 149° 52.5'E) from the northeastern tip it is at a depth of 2050 m (Figure 9). From this point the axis deepens to 2400 m at a southwestern tip one hundred and ten kilometers from the northeastern tip (Figure 10b).

The axis has a deviation from axial linearity (3° 17'S, 150° 07.9'E) 45 km behind its northeastern tip [Liu, pers.comm.,1988] (Figure 10b). To the northeast of the deviation from axial linearity the rift trends approximately 059° and to the southwest 044°. Hydrothermally altered, water rich, calc-alkaline rocks with high vesicularity were dredged from the northeastern extremity of this site [Sinton, pers. comm., 1988]. These characteristics are displayed by rocks dredged at deviations from axial linearity studied along the East Pacific Rise [Langmuir et al., 1986]. There is a seamount 6 km to the southeast of the axis that was generated at the deviation from axial linearity (Figures 9 & 10a).

Structural boundaries (Figure 11) are associated with the edge of the V-shaped region of normally magnetized crust. These boundaries are characterized by basement scarps that face both inward

towards the spreading axis and outward away from the spreading axis. The basement relief along the southeastern boundary ranges between 90 m and 330 m. The boundary is an inward facing scarp for the first 47 km of its length. It is an outward facing scarp as it encounters the southeastern flank of an off axis seamount and remains in this orientation as it approaches and crosses rough terrain associated with the southwestern boundary of the "transtensional zone". The extreme basement relief along these scarps results from the coincidence of the boundary with the wall of a graben (profiles 19 & 20, Figure 11), with the eastern flank of a seamount (profiles 22 & 23, Figure 11), and with rough terrain associated with the southwestern boundary of the alleged microplate (profiles 25 & 26, Figure 11).

In contrast, the northwestern boundary has more variation in scarp orientation, however, the range in basement relief is of the same magnitude as the southeastern boundary (Figure 11). The basement relief along this boundary varies between 35 m and 313 m. For the first 47 km it is an inward facing basement scarp. However, the scarp relief gradually diminishes due to burial by sediments until there is no surface expression at 54 km behind the tip and then re-emerges for the rest of the boundary length. The scarp turns outward facing at this point and remains in this orientation for the next 20 km after which (profile 25, Figure 11) it resumes an inward facing configuration for the remainder of its length. Therefore, not only do the boundaries change character along their respective lengths from inward to outward facing, but the range of their re-

spective basement reliefs is the same magnitude. The significance of the basement scarp orientations will commented upon in the discussion section.

Models

The tectonic setting outlined above, as well as the patterns in the magnetic data set (Figures 4, 5, 6, &7), suggest four end member models that could be applied and used to explain extension in the Manus Basin: a sphenochasm model, a propagating rift model, a microplate model, or a pull-apart model. The most notable magnetic feature, the V-shaped wedge of normally polarized crustal material centered over the northeast trending Manus Spreading Center (Figure 8), may be explained by either a sphenochasm model [Carey, 1958] or a propagating rift model [Hey et al., 1980, 1986, 1988]. The truncation of north-south trending magnetic lineations, both to the north by the V-shaped wedge of normally magnetized crust, and to the south by east-northeast trending short wavelength lineations associated with a pair of overlapping grabens (Figures 4 & 8), suggests that a microplate model ,either rigid or nonrigid, [Engeln & Stein, 1984, Engeln et al., 1988, Schouten et al., in prep.] may be appropriate in this area. In the southeastern portion of the basin a series of east-northeast trending magnetic lineations with normal polarity and short wavelength (Figures 4, 5, & 6) occur in the area

between the Djaul and Weitin transforms (Figure 8). This may be an area which is undergoing distributed stretching best described by a pull-apart model [Mann et al., 1983]. The following sections describe these end member models and their associated predictions. Subsequently, the magnetic data will be used to test which model, or combination of models, best fits the Manus Basin.

Sphenochasm Model

Carey [1958] proposed and defined the term sphenochasm as " a triangular gap of oceanic crust separating two cratonic blocks with fault margins converging to a point, and interpreted as having originated by the rotation of one of the blocks with respect to the other". There are several predictions made by the sphenochasm model in the context of the (subsequent) rigid plate tectonics hypothesis. The pole of rotation for the two crustal blocks is located at the end of the spreading ridge (Figure 12). The spreading rate increases monotonically along axis away from the spreading center tip. Magnetic lineations are fanned about the ridge and converge at the ridge tip. Fault zones border the crustal material generated by the ridge and the pre-existing crustal material. Outside these fault zones the same amount of pre-existing crustal material must be removed, either by distributed crustal shortening or by subduction.

Guided solely by geomorphological relationships Carey [1958] postulated the existence of a number of sphenochasms worldwide.One of his examples is the Woodlark Basin (Figure 1) which

Figure 12 Sphenochasm model. Light solid lines inside the ridge jump boundaries indicate structural lineations and isochrons. The dashed line shows the ridge axis. Compressional tectonic elements in pre-existing crustal material shown by fold and thrust or fold symbols. Pre-existing crustal material may be foreshortened by either localized folding (i.e. in strongly compressed zone)and thrusting or distributed crustal deformation (i.e. in weakly or moderately compressed zones)or destroyed by subduction (i.e. in a trench).

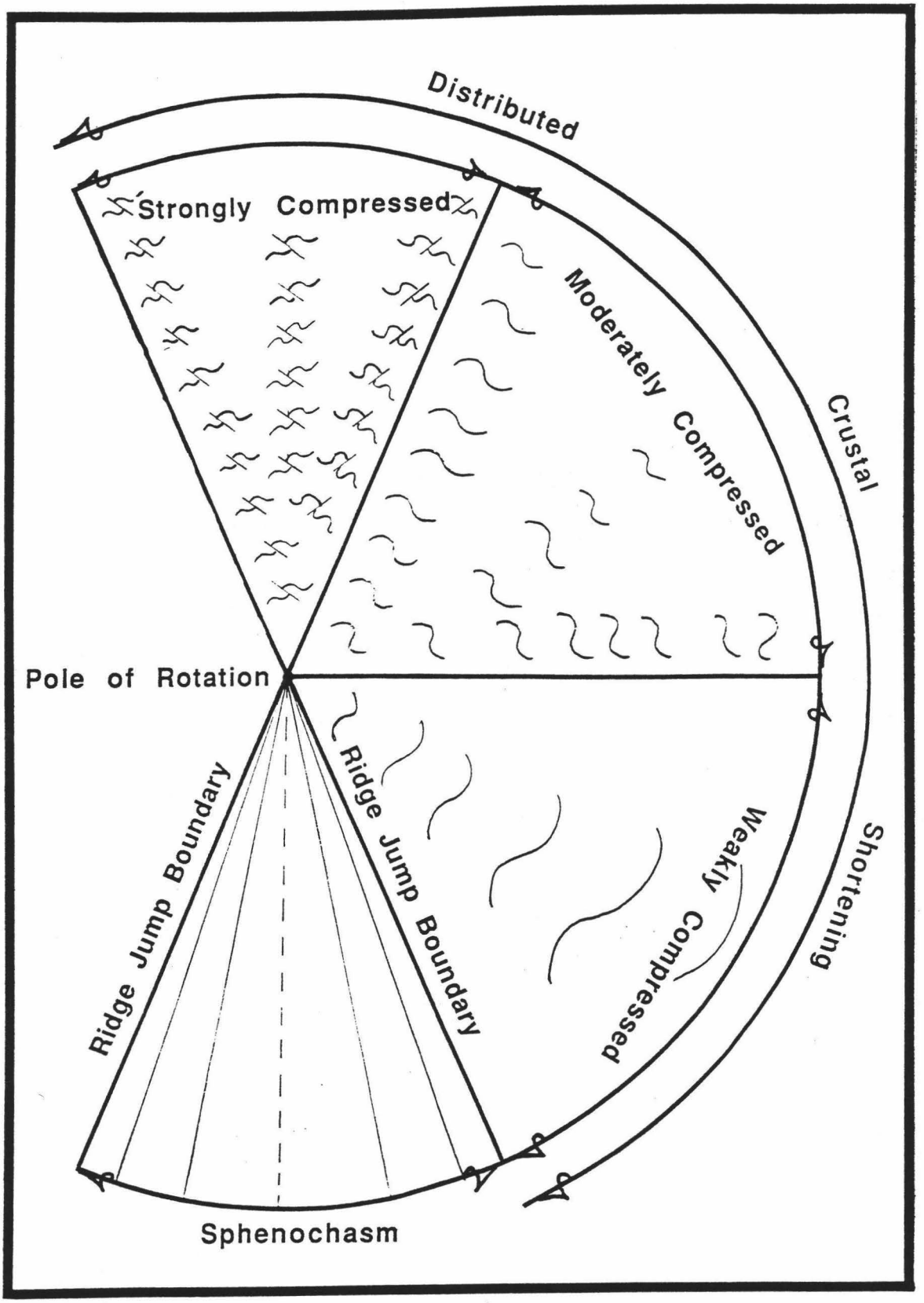
Distributed
Strongly Compressed
Moderately Compressed
Crustal
Shortening
Pole of Rotation
Ridge Jump Boundary
Ridge Jump Boundary
Weakly Compressed
Sphenochasm

he designated as the Louisiade Sphenochasm [Carey, 1958, his Figure 40b]. The pattern of magnetic anomalies supports a modified propagating sphenochasm model for the Woodlark Basin [Weissel et al., 1982, Hill et al., 1984, Taylor, 1987] the opening of which has been accommodated by northward subduction of the Solomon Sea plate at the New Britain Trench at a rate greater than 100 mm/yr [Johnson, 1979; Taylor, 1979].

Propagating Rift Model

Hey and colleagues developed the concept of propagating rifts [e.g. Hey et al., 1980, 1986, 1988] to explain data collected along the Galapagos spreading center. They have successfully applied this model to give simple explanations for complexities found in the Juan de Fuca [Hey and Wilson, 1982] and the Easter microplate areas [Hey et al., 1985]. Anomaly profiles in these areas commonly show departures from predicted symmetrical patterns with sporadic local sections of extra or missing anomalies. These types of perturbations in the lineations were originally ascribed to small ridge jumps [Hey et al., 1977]. Ridge jumps were thought to instantaneously move the center of spreading laterally to a new site, breaking a part off one plate and transferring it to the other. Rather, within the propagating rift model new ridges seem to incise themselves through existing crust at rates comparable to spreading rates. Propagation proceeds from the rift tip gradually overlapping and replacing the pre-existing spreading center. Understanding the

Figure 13 (A) Discontinuous, (B) continuous, and (C) broad transform zone oceanic propagation/failing rift models. Propagating rift lithosphere is marked by dark stipple, normal lithosphere created at the doomed rift is indicated by light stipple, and transferred lithosphere is cross-hatched. Heavy black lines show active plate boundaries. Figures 1A and 1B modified from Hey (1977) and Hey et al. (1980). In Figure 1C, modified from Mckenzie (1986), active axes with full spreading rate are shown as heavy black lines; active axes with transitional rates are shown as dashed black lines; transform zone is shown by white area. After Hey et al. (1988).

A) Discontinuous Propagation Geometry

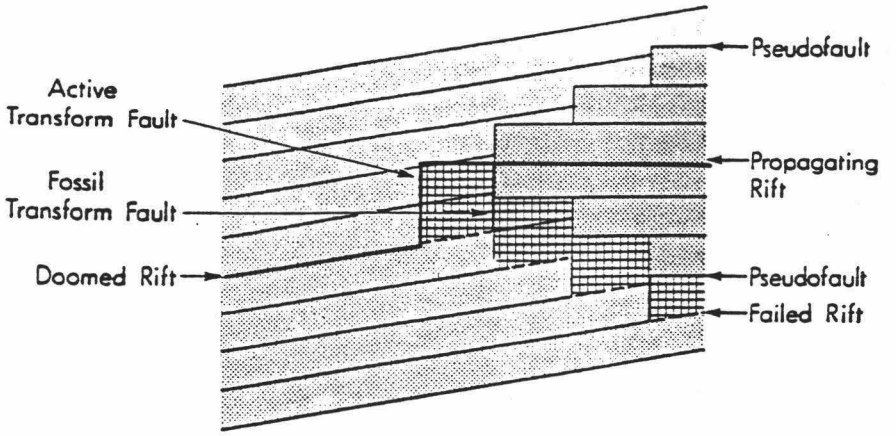

B) Continuous Propagation Geometry

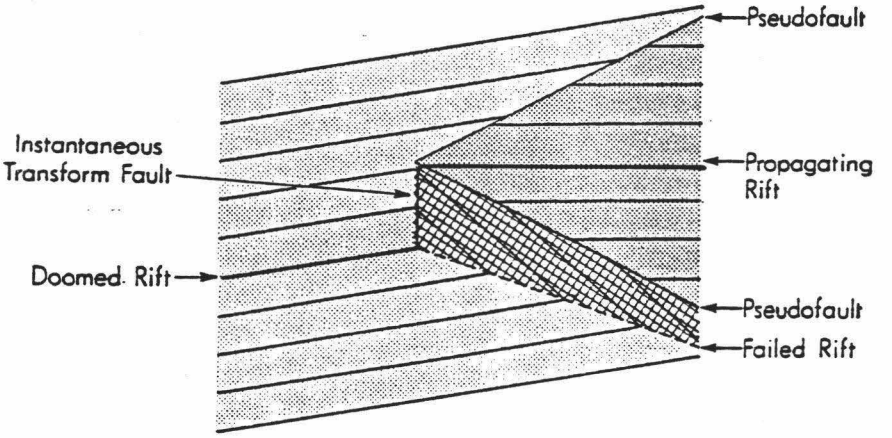

C) Broad Transform Zone Geometry

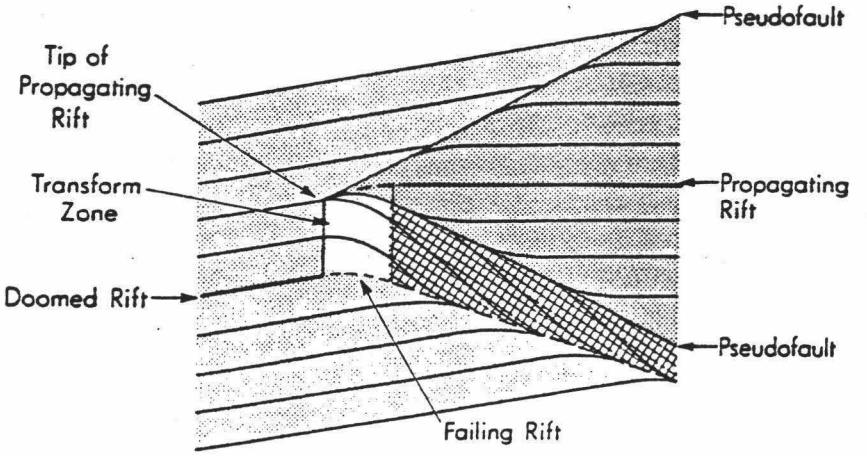

magnetic pattern created by the propagating rift may be facilitated by envisioning it in the discontinuous form (Figure 13a). Periodically, the propagating rift extends itself beyond the transform fault which connects the propagating and doomed rift tips and imbricates the existing rift. Active spreading switches to the annexed length and a new transform originates at its tip. In the broad transform zone version of this model (Figure 13c) the propagating rift is constantly lengthening at the expense of the doomed rift. In lieu of a single transform fault connecting the rift tips there is a broad transform zone. V-shaped magnetic anomaly traces are left by the propagating rift. The oblique V-shaped cicatrices are relics of the ridge propagation process which juxtaposed young oceanic crust against older lithosphere and are called pseudofaults [Hey, 1977]. The occurrence of high amplitude magnetic anomalies is also a phenomenon associated with propagating rifts. Christie and Sinton [1981] demonstrated that high amplitude magnetic anomalies are concomitant with ferrobasalts erupted behind the propagator tip. This is the result of a high degree of differentiation believed to be caused by low supply rates and moderate cooling rates before steady state magmatic processes are established. In essence Christie and Sinton propose that the magmas associated with the propagator tip undergo a closed-system fractionation in small unconnected chambers as the rift breaks through relatively older, cold lithosphere. There is a gradual transition to open-system magmatism as the magmatic plumbing becomes established behind the propagator tip. The resulting V-shaped geochemical boundaries are coincident with

the pseudofaults and high amplitude magnetic anomalies. These boundaries trace the past positions of the propagator tip and separate crust generated along the propagating rift from pre-existing 'normal' oceanic crust. With increasing distance behind the propagator tip the level of differentiation tapers off inwards from the pseudofaults reflecting the transition from a closed to an open magmatic system.

Predictions made by the propagating rift hypothesis are as follows. There is an instantaneous transform fault zone at the rift tip connected at its other end to some other plate boundary segment, commonly a failing rift/spreading center (Figure 13c). A V-shaped wedge of seafloor generated by the rift is bounded by pseudofaults marking past locations of the propagator tip. The wedge points in the direction of propagation. A ferrobasalt province extends as much as 50 km behind the rift tip and out along the pseudofaults. Scarps evidently forming during the initial rifting by normal faulting down towards the propagator axis locate the structural pseudofault zone [Kleinrock, 1988]. The spreading rate accelerates from zero to full rate over some finite time and distance on the propagating spreading center. Lastly, the magnetic lineations generated by the propagator are parallel to sub-parallel to the spreading axis and intersect the pseudofaults. The geochemical anomalies coincide with high amplitude magnetic anomalies and are bounded by the pseudofaults.

Microplate Models

Engeln and Stein [1984] and Engeln et al. [1988] have investigated possible kinematic models for the Easter plate region. They explored two cases which they hypothesize are limits of a continuum (Figure 14). They investigated a rigid plate and a shear zone in an overlap region. These end member cases are studied within the context of a propagating rift system. Their rigid plate model uses a three plate configuration. The Euler pole for the two large plates is 90° away. All spreading on the two bounding ridges is both orthogonal and symmetrical. Two different aspects of the microplates' history are reflected by the isochrons formed on the growing rift. The kinematics of rift propagation control the variation in age of the oldest seafloor bounded by and adjacent to the pseudofaults of the growing rift. The proximity of the microplate-large plate Euler pole yields a variation in the spreading rates along the growing rift and, hence, the spacing between isochrons increases with distance from the tip and from the pseudofaults to the axis. In the rigid case both effects augment producing a fanned anomaly pattern within the bounding pseudofaults. For the simple shear model, the entire overlap region deforms in simple shear parallel to the spreading direction as a response to the differential spreading along the two ridges. For the Galapagos 95.5°W propagating rift system the shear zone between the growing and dying rifts is not parallel to the slip vector between the plates [Hey et al., 1986]. Therefore, McKenzie [1986] has shown, the deformation zone is being stretched as well

Figure 14 (A) Rigid Microplate and (B) Shear Zone models. Double lines are spreading centers, single lines are transform faults, Arrows eminating from the spreading centers indicate spreading direction(s) and relative spreading magnitude(s). After Engeln and Stein, 1988.

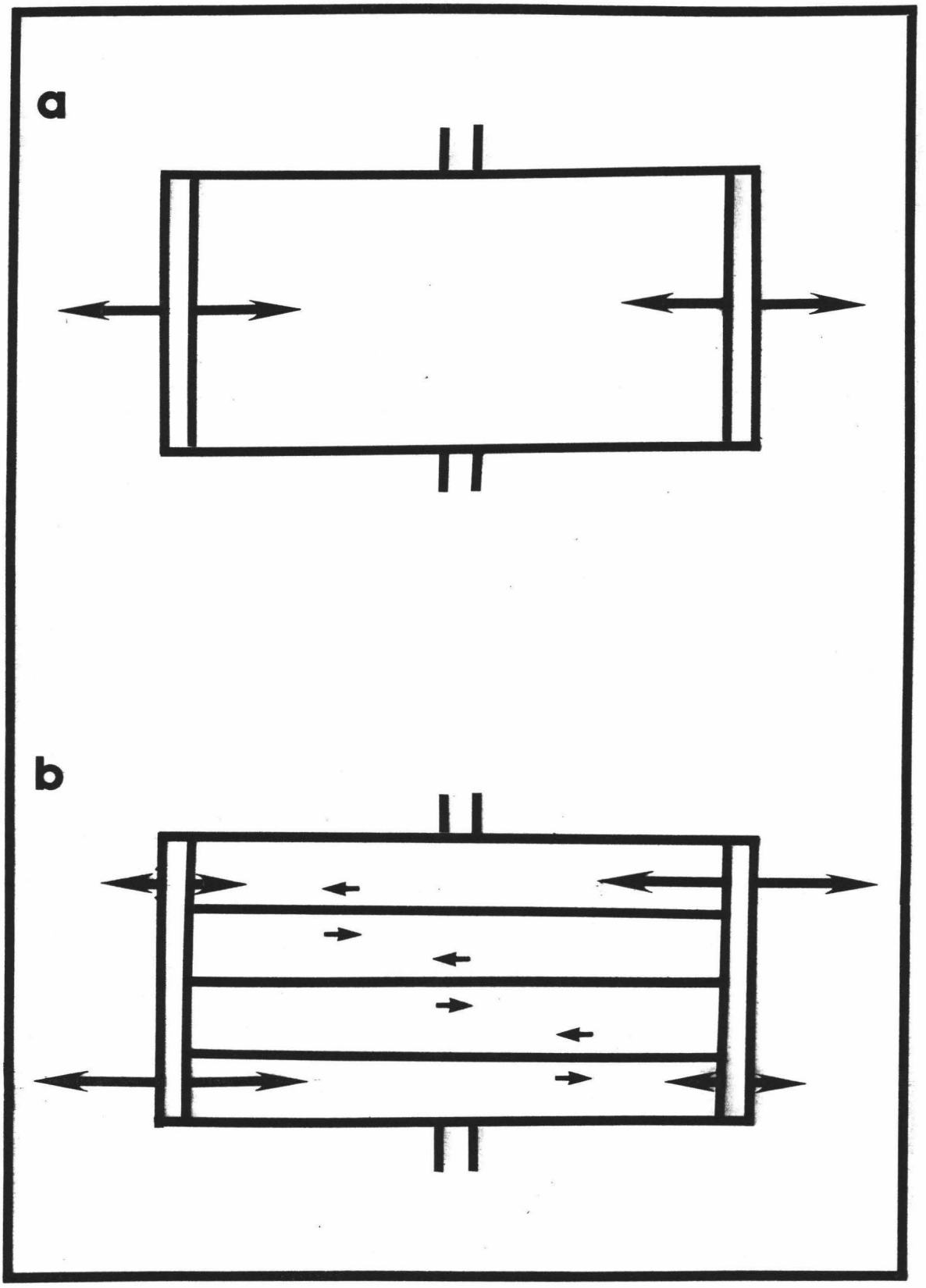
a
b

as sheared i.e. pure shear and simple shear [Hobbs et al., 1976] are occurring simultaneously. The differential translation and rotation of the seafloor reorients the isochrons within the overlap zone. In contrast, for the rigid case, isochrons within the microplate interior are reoriented by the transfer of seafloor at the microplate boundaries and by rigid rotation of the microplate. Therefore, the consequent oblique structure within the interior of the microplate/overlap region need not be the result of pervasive shearing. The rotation of a rigid microplate can produce similar, but not the same structural orientations. The greatest differences between the limiting cases can be seen in the evolution of the two non-ridge boundaries. In the case of a rigid plate one of these boundaries may become convergent i.e. compressive while the other could evolve into a slow spreading ridge. Both boundaries remain transforms in the shear model.

If second-order motions of a rigid microplate are considered [Schouten et al., in prep.], microplate motion can be adequately described by rotations relative to the surrounding plates. These rotations consist of two simultaneous rotations i.e. the motion of a point over the globe and a rotation about that point. An example of this second-order type motion would be that of a ball bearing (Figure 15). The instantaneous relative poles in the case of a microplate are located at or near the microplate boundaries and make up a constellation of unique points where the tangential microplate velocity about the microplate rotational axis equals the plate velocity relative to that same axis. It is at these points where the micro-

Figure 15 Ball bearing microplate model showing possible locations of the microplate rotational axis and the constellation of instantaneous relative rotation poles around the microplate boundary. After Schouten et al., in prep.

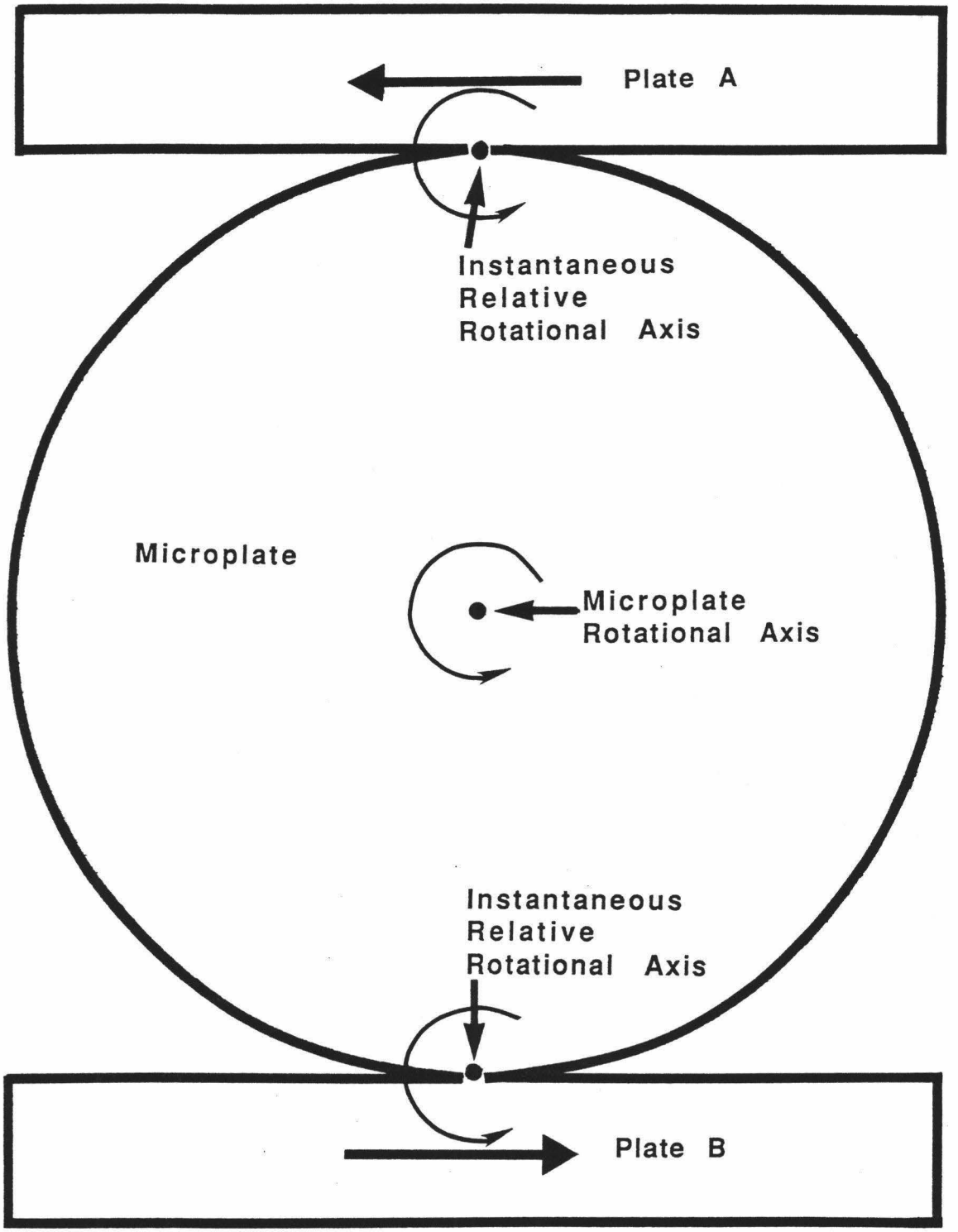
Plate A
Instantaneous
Relative
Rotational Axis
Microplate
Microplate
Rotational Axis
Instantaneous
Relative
Rotational Axis
Plate B

plate and adjacent plate(s) do not move relative to one another and where compression changes to extension along the microplate boundaries. These points migrate around the perimeter of the microplate as the microplate rotates and the adjacent plates move relative to one another. If the microplate rotational axis is located closer to one relative pole than to another then the velocity about the closer pole will be slower than about the more distant pole. In this way linear velocities about the constellation of instantaneous relative rotation axes can have widely disparate magnitudes. The microplate grows with time and immediately becomes unstable because propagation, extension, and accretion occur along the boundaries of the microplate [Hey, pers. comm., 1989]. The microplate becomes unstable in the sense that it may change shape and/or subsequently become attached to one of the adjacent larger plates [Hey et al., 1985, Anderson-Fontana et al., 1986].

Pull-Apart Models

In tracing the development of pull-apart basins Mann et al. [1983] reviewed several models proposed for this type of feature. In the simplest model [Crowell, 1974] a basin nucleates between two parallel side-stepped transforms (i.e. master faults) which step in the same sense as the offset along them (e.g. left-stepping left-lateral, Figure 16). The width of the basin is fixed and determined by the separation between the two master faults. As the overlap

Figure 16 (a) Extensional (minus) and compressional (plus) quadrants around a left lateral strike-slip fault; (b) rhomb graben on a left stepover; (c) normal faults (barbs on downthrown side) and major strike-slip segments with normal slip component bounding a rhomb graben at a left stepover. (After Aydin and Nur, 1982).

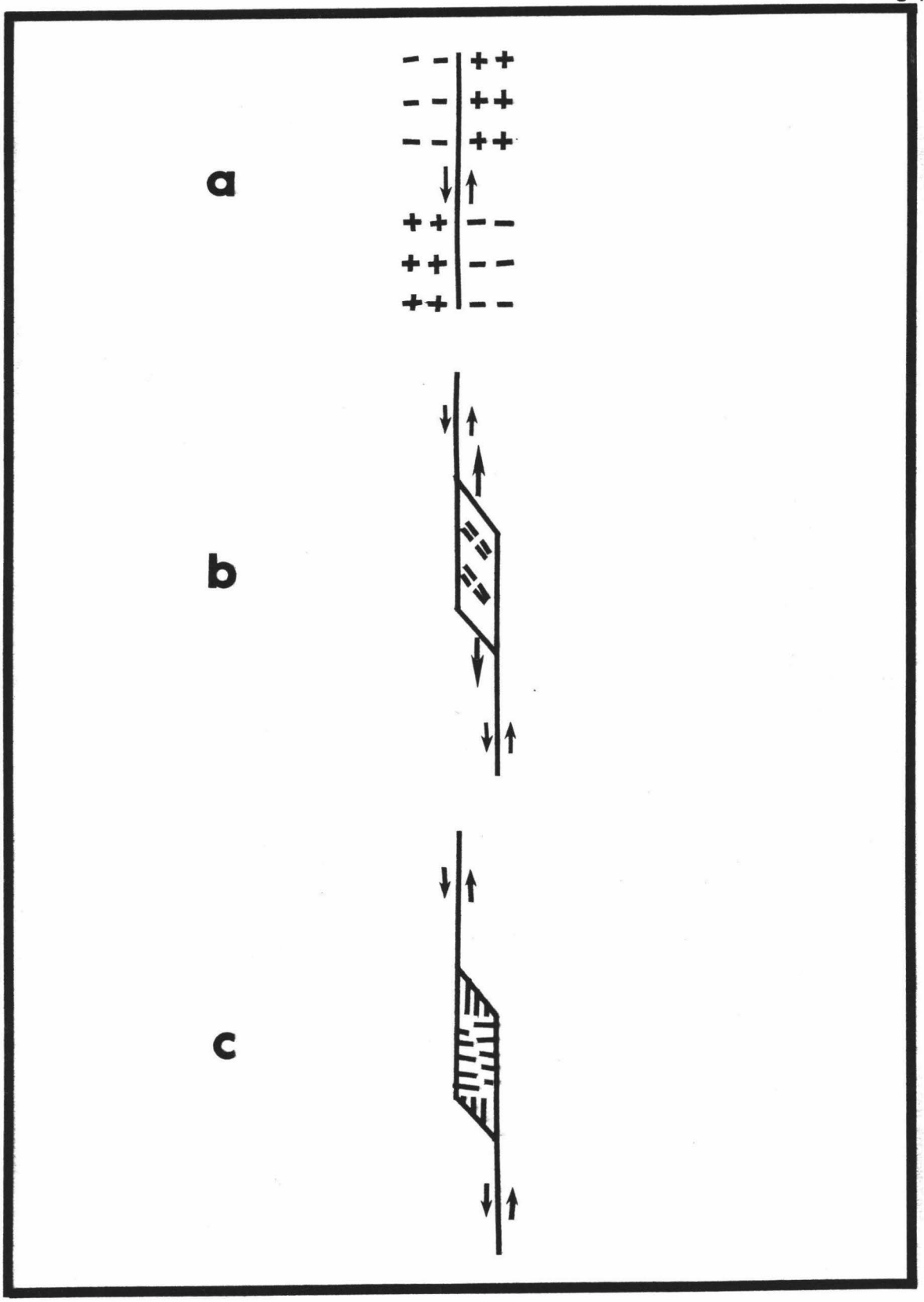
a
b
c

between the transforms increases so does the length of the pull-apart. The two sides of the depression bounded by the master faults have a significant amount of normal as well as strike-slip components (i.e. oblique-slip) [Aydin & Nur, 1982]. The other two sides are defined by predominantly dip-slip faults which trend diagonally to the transform faults. The secondary fault pattern established in the basin is complex, consisting of principally oblique normal faults trending approximately 35^{o} to 50^{o} to the master faults. Once the secondary fault pattern is established any further displacement on the master faults should produce movement on the previously formed fault pattern rather than creating any new patterns (even though the regional stress field might be substantially different at some later time).

Methods

To determine whether any of the above models adequately describes the tectonics occurring in the Manus Basin we performed forward and inverse modelling of the magnetic data.

Assumptions

There are three assumptions used for both the forward modelling and magnetic inversion programs. The sources are assumed to

be infinitely lineated perpendicular to the strike of the profile (two dimensional). The seafloor is modelled as a magnetized layer with a uniform thickness of 1 km and with the upper surface defined by the observed bathymetry. (The spatial distribution of the solution is not dependent upon the choice of layer thickness, although, the signal amplitudes scale almost linearly with layer thickness [Miller et al., 1985].) The assumption of a magnetized layer of uniform thickness is tantamount to assuming that most of the relief originated through faulting. It is assumed that the rock magnetization is uniform with depth.

Magnetic Forward Modelling

The first phase of this study used a computer package to forward model the magnetic anomaly profiles over the Manus Spreading Center. We used the program MAGBATH developed by Hey et al. [1986] and modified by Naar and Hey [1986] that constructs a Talwani-type parallelogram model and calculates the associated anomaly. The purpose of the forward modelling was to gain geological insight into the character of the Manus Spreading Center. We first identified central anomaly reversal boundaries present within the magnetic signal. From these, relative spreading rates and degree of asymmetric spreading were determined along the length of the Manus Spreading Center. Then we distinguished the occurrences of the Emperor reversed event [Wilson and Hey, 1981] on as many profiles as possible. This gave us absolute spreading rates for the pro-

files on which they occurred on both sides of the spreading axis. It was hoped that the magnetic anomaly isochron pattern would allow characterization of the Manus Spreading Center as either a sphenochasm [e.g. Carey, 1958] or a propagating rift [e.g. Hey et al., 1980, 1986, 1988].

The main modelling program uses the above assumptions and the magnetic polarity time scale of Kent and Gradstein [1986] (the Brunhes-Matuyama boundary is at 0.73 Ma and the Jaramillo event is at 0.91-0.97 Ma) modified to include the Emperor reversed event (.49-.50 Ma, [Wilson and Hey, 1981]) to produce a synthetic magnetic anomaly, which takes into account skewness of the magnetic anomaly resulting from the orientation and location of the ridge axis. The package as used here first computes the normal and reversed magnetic model. At the next stage the model is merged with the bathymetry data. The magnetic anomaly is then computed. The final programs in the package plot the results (Figure 7), which consist of the magnetic data (top profile), the magnetic model (middle profile), and the associated reversal block model superimposed on bathymetry (lower profile). The present day spreading axis as defined by the bathymetry and sidescan was used to locate the model axis.

Magnetic Inversion

Parker and Huestis [1974] introduced the two-dimensional inverse method to marine geological and geophysical data. Since then

it has been applied to a substantial collection of magnetic profiles [e.g. Klitgord et al., 1975, Macdonald, 1977, Macdonald and Holcombe, 1978, Miller et al., 1985]. Inversion produces a crustal magnetization distribution free of the contamination of bathymetry effects and of skewness. We used the two-dimensional inverse program INV2D developed by Miller et al.[1985] that uses the common set of assumptions above to compute a model with magnetization allowed to vary horizontally along profile. The inputs to the inversion are the observed field and bathymetry along profile and the appropriate International Geophysical Reference Field. Outputs from the inversion are a magnetization distribution and the annihilator. The computed distribution reproduces the observed field anomaly in the presence of bathymetry.

The crustal magnetization derived from the inversion is nonunique even with the above assumptions. Solutions may be found for the inverse problem for any choice of direction of magnetism, direction of ambient field or thickness of magnetic layer. An understanding of the nonuniqueness of the inverse problem can be gained through characterization of the 'annihilator' function. The annihilator has been defined as the horizontal magnetization distribution that produces no external field for a given topography. Because the annihilator produces no external field, any amount of it can be added to the original solution of the inverse problem. The summed solution will also produce the observed field. Addition of the wrong amount of annihilator can create artificial accelerations and decelerations in seafloor spreading rates when fast and slow spreading are cor-

related with positive or negative polarities. The 'appropriate' amount of annihilator is derived from the geological side constraint that positive and negative fluctuations of the solution should have approximately equal magnitudes when major magnetic reversals are crossed.

The inversion of magnetic anomalies amplifies the high and low wave numbers much like downward continuation. Therefore, high- and low-pass filters with cosine tapers were used to suppress this amplification while minimizing the effect of the side lobes on the data. The reason for the basic instability of the magnetic inverse problem can be seen if we view the nature of the forward problem, which is a smoothing operator. The forward computation of the magnetic field intensity on a plane a given distance above the sources smooths out the short wavelength variations in the source magnetization distribution. The opposite is true with the inverse problem. The magnetic solution amplifies the short wavelength variations in the input (observed) field data. The seafloor topography is almost entirely responsible for the short wavelength signal. The signal is dominated by the top of the magnetic layer and essentially unaffected by the bottom of the magnetic layer. Each iteration of the inversion process is low pass filtered to prevent oscillation of the solution at short wavelengths; as a consequence, each recomputed field is slightly smoother than the input observed field.

Magnetic Interpretation

Figure 4 shows the magnetic anomaly profiles along track within the survey area. The data are hand contoured in figure 5. The warm colors in this figure are positive magnetic values while the cool colors indicate negative magnetic values. When looking at the area between 149°E and 150° 30'E in these figures the most striking features are the northeast trending V-shaped wedge of normally polarized crust situated over the Manus Spreading Center and the east-west bearing negative anomaly lineations over the "extensional transform zone" that trend away from the southwestern end of the V-shaped crust and that also correspond to normally magnetized crust. Material within the V-shaped boundaries is modelled to have been generated by the Manus Spreading Center during the Brunhes chron. The locations and trends of the lineations created by the occurrences of the Emperor reversed event inside the V-shaped boundaries are indicated by heavy dashed lines (Figure 4). The normally polarized crustal material that strikes east-west away from the southwestern end of the Manus Spreading Center has been generated by the overlapping, right stepping en echelon spreading segments comprising the "extensional transform zone" during the Brunhes chron. This may be an area of overlapping short northeast-southwest trending magnetic lineations. However, since the data were collected at the sea surface (i.e. approximately 2 km above the source) we are not able to resolve these magnetically. Examination

of the region to the northwest of the Manus Spreading Center and north of the "extensional transform zone" reveals an area of high amplitude magnetic anomalies (Figure 4) bounded on the south and southeast by an extreme gradient (Figure 5). Peak to peak amplitude values exceed 1800 nT in this zone. To the southeast of the Manus Spreading Center in the "transtensional zone" interior the anomalies are more subdued and the dominant magnetic trend is north-south. This fabric is truncated to the south by crust generated on the southern overlapping rift grabens. These "transtensional zone" lineations, whose north-south orientation suggests counterclockwise rotation of the crust, are truncated by lineations generated on the bounding extensional segments . The anomalies over the rift grabens, and over the en echelon ridges between the Djaul and Weitin transform faults, are of low amplitude and short wavelength (7-15 km). The short wavelength character of these anomalies may be the result of either slow spreading or a short pulse of fast spreading. Limited east-northeast trending lineations are associated with both the rift grabens and the en echelon ridges.

The same features seen in figures 4 and 5 are also present in figure 6 showing the crustal magnetization for the survey area. The main feature is again the northeast trending wedge of normally magnetized material. At the boundaries of the V-shaped wedge of normally magnetized crust approximately 60 km behind its northeastern tip (near 3° 23'S, 150° 02'E) the magnetization amplitudes are higher than in the interior of the wedge. This suggests the presence of ferrobasalts of even higher magnetization than the axial basalts, as

seen in areas of propagating rifts such as the Galapagos at 95° 30'W [Sinton, et al., 1983] and the Easter microplate [Schilling et al., 1985]. Alternatively the inferred ferrobasalts may mark the sites of initiation of spreading following a ridge jump into an area undergoing transtension and possibly associated with low magma supply rates and moderate cooling rates that would prevail while an open magmatic plumbing system was being established. The high magnetization amplitudes observed in the area northwest of the Manus Spreading Center are not explained by either of the above models. While not as well defined in this figure, the north-south magnetic trends in the interior of the "transtensional zone" can again be seen as can their truncation by crust generated on the Manus Spreading Center and the southern rift grabens. Low amplitude, short wavelength central anomalies are associated with the rift grabens south of the Manus Spreading Center and the en echelon ridges in the southeastern part of the basin. The spreading center locations within the central anomaly correlations are indistinct for these two areas, which could be the result of crustal stretching rather than localized spreading.

Figure 7 shows the results of forward modelling of magnetic profiles. Having limited model constraints we projected the magnetic profiles perpendicular to the trend of the central Manus Spreading Center (i.e. perpendicular to 044°). The figure shows a widening of the central anomaly as one progresses from the northeastern rift tip towards the southwest along the axis. The boundaries of the central anomaly have been modelled to mark the limits

of the crust generated by the Manus Spreading Center. No attempt was made to model recent rift jumps within these boundaries. Rather, asymmetry was used to match what could be attributed to either asymmetric spreading or asymmetric accretion [Hey et al., 1977] (Figure 7). All profiles have only been modelled out to the ridge jump boundaries. Model spreading rates increase monotonically away from the northeastern rift tip towards the southwest reaching a maximum of 114 mm/yr full rate. Emperor reversed events [Wilson & Hey, 1981] occur on profiles 23 and 24 (south side only), and profiles 25 and 26 (both sides). Ridge jump times were calculated by extrapolating the spreading rates from matching the Emperor reversed events to the edge of the Brunhes. This suggests that a ridge jump established the spreading center at its present southwestern end. The central anomalies and forward models appear symmetric because the ridge jumped into predominately reversely polarized crust except where north-south trending normally polarized lineations intersect the southeast central anomaly boundary. The symmetry of the profiles also implies oblique symmetric spreading in the trackline direction which fortuitously is the transform direction (i.e. approximately 119^{o}). The maximum spreading rate in this direction is 118 mm/yr. Using the crustal generation values for profiles 25 and 26 (Figure 10c) we calculate a ridge jump event at .68 Ma. Anomalies outside the boundaries are difficult to identify probably due to local tectonic complexities. These complexities may have been introduced by rotation and by simple shear [McKenzie and Jackson, 1983] of crustal material

within the interior of the "transtensional zone" as a result of crustal generation on the Manus Spreading Center and the southern rift grabens. Anomaly amplitudes along the northwestern boundary are high and show an extreme gradient while anomalies along the southeastern boundary are more subdued. As was pointed out above the basement relief along these boundaries changes somewhat randomly and the scarps alternate between facing towards the neovolcanic zone and facing away from it. Thus bathymetry does not help in explaining the differences in anomaly amplitudes northwest and southeast of the Manus Spreading Center central anomaly.

All the models in figure 7 show a reasonable fit to the data out to the ridge jump boundaries with the exception of profile 17 (Figure 7a). It was found that 45% asymmetry was needed to match the data for this profile. Since this is an unrealistic amount of asymmetry we chose a symmetric model about the graben based on the SeaMARC II imagery and used the bathymetry to establish reasonable sites for the ridge jump boundaries. Therefore a positive piece of crust would need to be added to the southeast in order to make the model more realistic. Normally we would be able to do this using the ridge jump parameter in the modelling program. However, since we as yet have no definite site for prior spreading in the basin (although we strongly suspect it to be in the western portion of the Manus basin), we were unable to do this. The magnetic data are missing for the northwest portion of profile 22 (Figure 7f) because of a magnetometer malfunction. We assumed symmetrical spreading for this profile

and therefore, the position of the northwest boundary of crustal generation on this trackline may not be accurate.

Discussion

Several models have been proposed for extension in back-arc basins. At one end of the continuum are models which envision extension being accommodated on spreading segments analogous to mid-ocean ridges [Weissel, 1981, Uyeda, 1986]. At the other end are models appealing to disorganized back-arc extension, characterized by abundant short-lived spreading ridges and point source volcanism as major components [Lawver et al., 1976, Lawver & Hawkins, 1978, Hamburger & Isacks, 1988]. There are elements of both these end-member models present in the New Britain back-arc where the extensional boundaries are both rapidly evolving and spatially localized. The model that we believe best describes the lithospheric accretion currently taking place in the Manus Basin is one in which crustal extension is occurring in a transtensional environment between left-stepping, left-lateral transforms. The following paragraphs describe the extensional segments moving from west to east across the basin and argue for the existence of tensional environments between the transform segments.

While our magnetic data do show an east-west swath of normally magnetized crustal material between 148° 54'E and 149° 48'E

over the "extensional transform zone" (Figures 4, 5, and 6), they do not constrain either the spreading rate(s) or direction within this zone. However, since the spreading on the overlapping, en echelon ridge segments has generated enough normally magnetized crust to match the fast spreading at the southwest end of the Manus Spreading Center, the total spreading rate (118 mm/yr) must be the about the same in both places. The spreading direction is parallel to the strike of the Willaumez and Djaul transforms and crustal generation has been measured along this azimuth. As described earlier, the "extensional transform zone" is composed of short right stepping en echelon spreading segments (8 to 29 km long) cut by a Riedel shear. The magnetic lineations should mimic the structural trend(s) and/or be perpendicular to the spreading direction, however, the short wavelength signal generated by spreading on the ridges has been filtered out by the time it reaches a sensor at the sea surface. Therefore, the magnetic lineations can only be resolved to an east-west orientation by us (Figure 5).

The main extensional tectonic feature in the basin is the Manus Spreading Center comprising the northwestern boundary of the "transtensional zone". The spreading segment is sigmoidally shaped, possibly reflecting a passive response to the sinistral shear motion along the plate boundary through the basin. The magnetics constrain the time and location of the ridge jump which caused this extensional segment to be incised at or near its present location. Whether the ridge started spreading along the entirety of it's present length (i.e. sphenochasm) as modelled above or propagated

northeast from somewhere in the area of the "extensional transform zone" (i.e. propagating rift) cannot be determined from the magnetics alone. While the occurrences of the Emperor reversed event do form short lineations appearing to converge towards the northeastern tip inside the V-shaped boundaries, their length prevents confidence in extrapolation of this apparent convergence to it's point of intersection at the tip. Were we able to extrapolate a convergence of the magnetic lineations within the V-shaped boundaries, a sphenochasm for the Manus Spreading Center would be strongly indicated. If the Manus Spreading Center is a sphenochasm, approximately 3300 km^2 of crustal material would have to be accounted for by crustal shortening or by subduction. The crustal shortening would have to be either distributed in areas juxtaposed to the spreading segment (including the region opposing and to the northeast of it) or concentrated along one of the plate boundaries. The SeaMARC II imagery (Figure 8a) and bathymetry (Figure 9) fail to show any evidence to support the required crustal shortening. Further, there is no evidence for any sizable amount of subduction along the Djaul fault which is the most likely site for this to occur. The lack of any compressional seismicity along the fault and the ubiquity of strike-slip mechanisms throughout the basin also argues against subduction (Figure 2). Alternatively, a propagating rift for the Manus Spreading Center would be strongly indicated if magnetic or structural lineations inside the V-shaped boundaries intersected them. While the propagating rift model does not mandate a failing rift system, one would be required for a propagator operating in the

basin today based on paleomagnetic data [Falvey and Pritchard, 1985] indicating that Manus backarc spreading has existed since the Pliocene. Bending of the northeastern tip of the Manus Spreading Center to the east-southeast precludes the existence of a failing rift system in the western part of the Manus Basin, and the nature of the southern rift grabens does not make them a likely candidate for a failing rift system. As was mentioned earlier this is an area associated with short wavelength magnetic anomalies where there is only an indistinct correlation of central anomalies with the present locations of lava extrusion i.e. in the grabens. This indicates an area that is presently undergoing stretching via transtension and not a localized spreading system that is failing.

If a ridge jump into a transtensional environment were the sole tectonic process responsible for the evolution and present configuration of the Manus Spreading Center we would expect to see a maximum in crustal generation at some midpoint between the extremities of the spreading segment with a concomitant tapering off of crustal generation towards the bounding transforms [Ramsay, 1967]. Instead we see a maximum in crustal generation at the southwestern end of the Manus Spreading Center and a minimum at its northeastern end (Figure 10c). If a sphenochasm following a ridge jump was the lone process responsible for the crustal generation, the proximity of the Euler pole would require compression against the Djaul transform. As was stated above none of the data show this. Therefore, we prefer a scenario which incorporates both the sphenochasm and propagating rift models. Within this context

we envision the Manus Spreading Center being established via a ridge jump at .68 Ma along a distance a few kilometers less than it's present length (Sylvester, 1988, his Figure 30). Subsequently, several rigid blocks of crustal material within the overlap zone between the transform faults rotated (in the sense of McKenzie and Jackson, 1983), and the ridge propagated a few kilometers to the northeast.

Southeast of the central spreading segment the next area which is accommodating extension is bounded on the south by a pair of east-northeast trending overlapping grabens. The morphology of these extensional rift segments supported by the freshness of the lavas in the grabens, the lack of sediment cover, and the short wavelength normal polarity magnetic anomalies over the grabens constrains this to be a recent pulse of spreading. Spreading rates on these segments are probably an order of magnitude slower than that of the Manus Spreading Center. The absence of ridge construction within these grabens may be the result of a low magmatic budget which fails to keep pace with extension [Sinton et al., 1986].

In the southeastern portion of the basin between the Weitin and Djaul transforms, the east-northeast trending en echelon spreading segments occupy a graben between the two transforms. Crustal stretching is distributed over the overlap region between the transforms but the volcanism is concentrated on the spreading segments. Their sigmoidal shape points to a passive response to crustal stretching parallel to the transform faults. The ridges may be the result of a magma supply which has recently begun to keep

pace with the crustal stretching. The basaltic lavas form large flow fields whereas the more siliceous lavas (calc-alkalic island arc associated rocks, [Liu pers. comm., 1989]) form ridges. The freshness of the lavas, the lack of sediment cover though near the eastern edge of the basin and landmasses, and the short wavelength normal polarity magnetic anomalies over these spreading segments constrain the spreading to be a recent extensional event . Further, Taylor [1979] determined the location of a best fitting pole of relative motion between the Pacific and Bismarck plates to be at 18° 30'S, 141°E. As mentioned before the "extensional transform zone" is located on the Pacific/Bismarck plate boundary and is spreading with a total rate which is the same order of magnitude as the southwestern end of the Manus Spreading Center. Since the en echelon ridges are situated along the same Pacific/Bismarck boundary but farther away from the pole of rotation for these two plates, their total spreading rate must be at least the extensional transform rate and should in fact be somewhat faster. Therefore, not only is the spreading event here recent as evidenced by the short wavelength magnetic signals but it is happening at a rapid rate.

As mentioned in the models section the magnetics data seem to indicate the existence of a microplate in the basin. The magnetic lineations (Figure 5 & 6) as well as the structural (Figure 8b) and bathymetric (Figure 9) lineations strike northeast within the V-shaped wedge of normally magnetized crust while these same types of lineations trend north-south within the interior of a proposed microplate [Taylor et al., 1987]. This information coupled

with the differential spreading along the Manus Spreading Center (i.e. monotonically increasing from northeast to southwest) imply counterclockwise rotation of the plate. A rigid microplate model would explain the somewhat S-shape of the Djaul transform (Figure 8b). A rigidly rotating microplate could require the northwestern portion of the Djaul transform to have a component of extension across it, bowing it to the southwest, while the southeastern end would have a component of compression across it, thus bowing it to the northeast. However, a model incorporating rotating rigid crustal blocks in an overlap zone would also explain the transform's shape. Evidence for compression across the southeastern portion of the Djaul Transform can be seen in figure 9 where a bathymetric high at 3° 32'S, 151° 09'E abuts the fault. We interpret this feature to be a compression ridge having the correct dimensions to have resulted from the collision of a crustal block with the transform boundary. Evidence for nonrigid deformation in the overlap zone between the Djaul transform and the proposed southwestern transform boundary to this zone comes from focal mechanism solutions for earthquakes occurring in the interior of the region that have nodal planes parallel to the northeastern boundary (Figure 2). If these earthquakes involved oblique slip motion on pre-existing structural lineaments, then rotation as proposed by McKenzie and Jackson [1983] would be occurring and the parallel alignment of the nodal planes with the northeast boundary would be compatible. Alternatively, right lateral strike-slip motion could be occurring on the nodal planes perpendicular to the strike of the Djaul transform. However, this

would require either localized spreading of equal magnitude at the boundaries of the region under tension if the crustal blocks extended over the full length of the overlap zone [Jackson & McKenzie, 1983, Lamb, 1988] or, if the dimensions of crustal blocks being rotated were smaller, a series of en echelon spreading segments would have to be established across the overlap region. Since the data do not indicate that either of these scenarios exist here we opt for the oblique slip explanation.

An overall model for the basin emerges which is dominated by left-lateral shear between the Pacific and Bismarck plates (Figure 17). Extension along this boundary is a left-stepping passive response to the shear and occurs on various types of extensional segments sharing a common sigmoidal shape. Spreading on the Manus Spreading Center is localized with crustal generation increasing monotonically from northeast to southwest. Extension on the "extensional transform zone" and the southeastern rifts segments is distributed throughout each of these zones, although, volcanism is concentrated on the spreading segments. Total spreading rates on these segments are the same order of magnitude as the fast spreading southwestern end of the Manus Spreading Center. A "transtensional zone" exists between the Manus Spreading Center and the southern grabens and the Djaul transform and a proposed southwestern transform boundary. The spreading rate on the southern grabens is probably an order of magnitude less than that of the Manus Spreading Center. However, the spreading is augmented by crustal stretching and, therefore, the total extension across the

Figure 17 Simplified tectonic model for the Manus Basin. Small arrows indicate spreading direction. Large arrows indicate relative plate motion. Barbs are on the downthrown sides of faults and ridge jump boundaries.

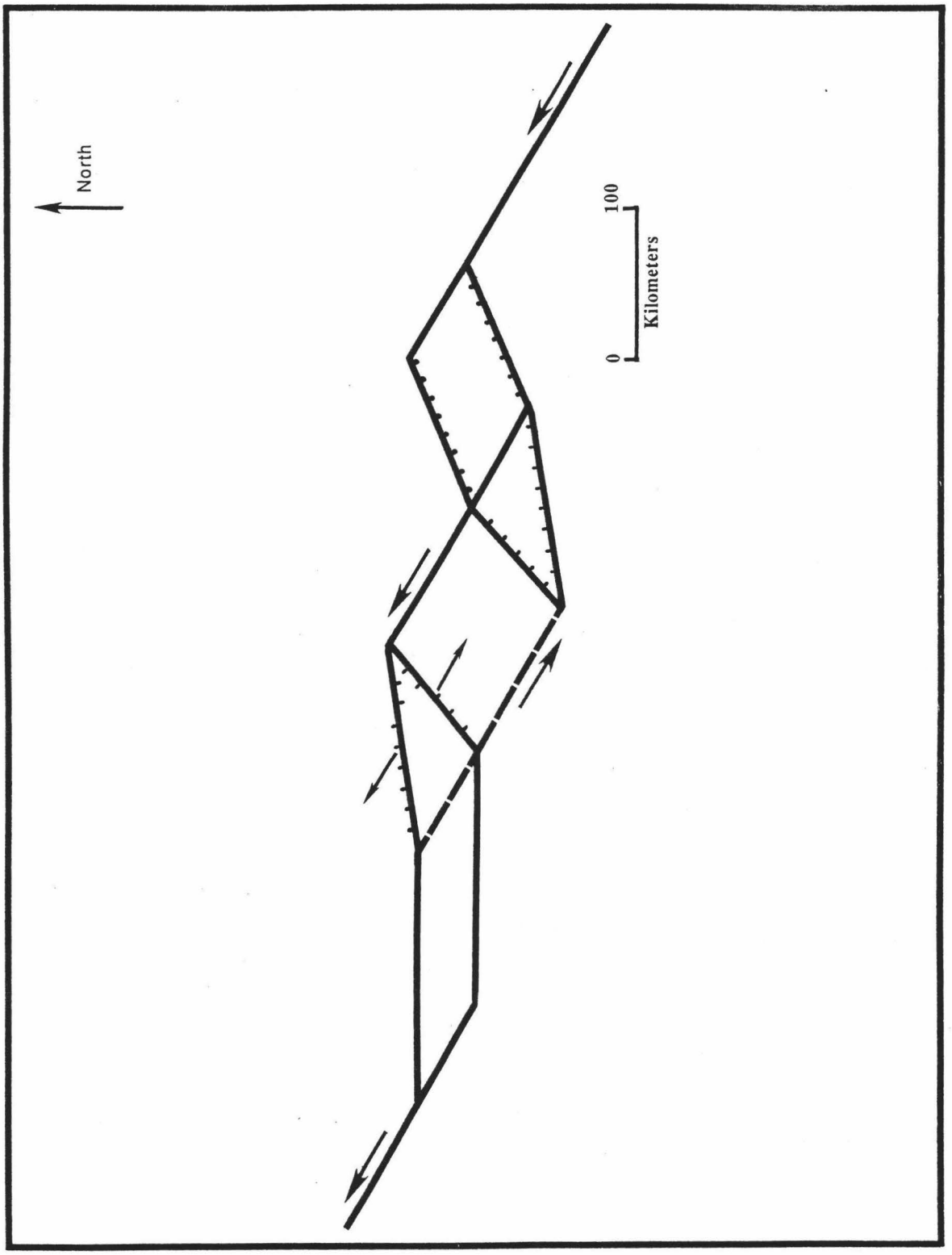
North
100
0
Kilometers

eastern end of these grabens is of the same magnitude as on the southwestern end of the Manus Spreading Center. Rigid crustal blocks within the "transtensional zone" have rotated counterclockwise in response to the differential spreading/stretching on its two extensional boundaries and the shear couple between its two transform boundaries.

Conclusions

A tectonic model has been developed for the Manus basin in which left lateral shear between the Pacific and Bismarck plates predominates. Extension occurs along several plate boundary segments as a passive response to this sinistral shearing motion. Forward modelling has shown that crustal generation along the Manus Spreading Center increases monotonically away from its northeastern ridge tip reaching a magnitude of 118 mm/yr full rate near its southwestern end. The magnetics data have allowed us to establish the locations and strike of the ridge jump boundaries for this spreading segment. The time of the ridge jump at the southwestern end of the Manus Spreading Center has been determined to be .68 my. The magnetics data help establish the existence of a 1200 km^2 "transtensional zone" that is being stretched and rotated between four active boundaries: the Djaul transform, a proposed southwestern bounding transform, the Manus Spreading Center, and the

southern grabens. The data have shown that the magnetic lineations inside the ridge jump boundaries are striking approximately north-east, while the lineations to the southeast in the "transtensional zone" trend north-south. This difference in lineation trends coupled with bathymetric and structural information constrains the rotation direction of the crustal material to be counterclockwise. The magnetic lineations associated with the southeastern ridges and southern grabens are narrow and of normal polarity. The freshness of the lavas and lack of sediment cover augment the magnetics data in constraining spreading on these extensional segments to be recent events. The total extensional rate on the southern grabens is probably the same order of magnitude as that occurring on the southwestern end of the Manus Spreading Center. The total spreading rate over the southeastern rifts is probably the same order of magnitude as that occurring over the "extensional transform zone". The resolution of the magnetic data is not good enough for us to constrain either the spreading directions or rates on the short en echelon ridges within the extensional transform zone. However, spreading on the extensional transform ridge segments has generated enough normally magnetized crust to match the fast spreading at the southwest end of the Manus Spreading Center (118 mm/yr).

References

Anderson-Fontana, S., J. Engeln, P. Lundgren, R. Larson, and S. Stein, Tectonics and evolution of the Juan Fernandez microplate at the Pacific-Nazca-Antarctic triple junction, J. Geophys. Res., 91, 2005-2018, 1986.

Aydin, A., and A. Nur, Evolution of pull-apart basins and their scale independence, Tectonics, 1, 91-105, 1982.

Both, R., K. Crook, B. Taylor, S. Brogan, B. Chappell, E. Frankel, L. Liu, J. Sinton, and D. Tiffin, Hydrothermal Chimneys and Associated Fauna in the Manus Back-Arc Basin, Papua New Guinea, EOS Trans. AGU, 67, 489-490, 1986.

Carey, S., A Tectonic Approach to Continental Drift, Univ. of Tasmania Geol. Dept Publ., 59, 177-355, 1958.

Christie, D., and J. Sinton, Evolution of Abyssal Lavas along Propagating Segments of the Galapagos Spreading Center, Earth. Planet. Sci. Lett., 56, 321-335, 1981.

Coleman, P., and G. Packham, The Melanesian borderlands and India-Pacific plates' boundary, Earth Sci. Rev., 12, 197-233, 1976.

Connelly, J. B., A Structural Interpretation of Magnetometer and Seismic Profiler Records in the Bismarck Sea, Melanesian Archipelago, J. Geol. Soc. Aust., 21, 459-469, 1974.

Connelly, J. B., Magnetic and Gravity Modelling in the Bismarck Sea (abstract), Bull. Aust. Soc. Explor. Geophys., 6, 52, 1975.

Connelly, J. B., Tectonic Development of the Bismarck Sea based on Gravity and Magnetic Modelling, Geophys. J. R. Astr. Soc., 46, 23-40, 1976.

Cooper, P. A., Seismicity, focal mechanisms and morphology of subducted lithosphere in the Papua New Guinea-Solomon Islands region, Ph. D. dissertation, 197pp., University of Hawaii at Manoa, 1985.

Craig, H., and R. Poreda, Studies of Methane and Helium in Hydrothermal Vent Plumes, Spreading-axis Basalts, and Volcanic Island Lavas and Gases, in Southwestern Pacific Marginal Basins, SIO Reference 87-14, pp. 37-43, University of California Scripps Institution of Oceanography, 1987.

Crowell, J., Origin of late Cenozoic basins in southern California, in Dickinson, W. R., ed., Tectonics and Sedimentation: Society of Economic Paleontologists and Mineralogists Special Pub. No. 22, pp. 190-204, 1974.

Connelly, J. B., A Structural Interpretation of Magnetometer and Seismic Profiler Records in the Bismarck Sea, Melanesian Archipelago, J. Geol. Soc. Aust., 21, 459-469, 1974.

Connelly, J. B., Magnetic and Gravity Modelling in the Bismarck Sea (abstract), Bull. Aust. Soc. Explor. Geophys., 6, 52, 1975.

Connelly, J. B., Tectonic Development of the Bismarck Sea based on Gravity and Magnetic Modelling, Geophys. J. R. Astr. Soc., 46, 23-40, 1976.

Cooper, P. A., Seismicity, focal mechanisms and morphology of subducted lithosphere in the Papua New Guinea-Solomon Islands region, Ph. D. dissertation, 197pp., University of Hawaii at Manoa, 1985.

Craig, H., and R. Poreda, Studies of Methane and Helium in Hydrothermal Vent Plumes, Spreading-axis Basalts, and Volcanic Island Lavas and Gases, in Southwestern Pacific Marginal Basins, SIO Reference 87-14, pp. 37-43, University of California Scripps Institution of Oceanography, 1987.

Crowell, J., Origin of late Cenozoic basins in southern California, in Dickinson, W. R., ed., Tectonics and Sedimentation: Society of Economic Paleontologists and Mineralogists Special Pub. No. 22, pp. 190-204, 1974.

Curtis, J. W., Plate Tectonics and the Papua-New Guinea-Solomon Islands region, J. Geol. Soc. Aust., 20, 21-36, 1973.

Denham, D., Distribution of Earthquakes in the New Guinea-Solomon Islands Region, J. Geophys. Res., 74, 4290-4299, 1969.

Dziewonski, A., and J. H. Woodhouse, An experiment in systematic study of global seismicity: centroid-moment tensor solutions for 201 moderate and large earthquakes of 1981, J. Geophys. Res., 88, 3247-3271, 1983.

Eguchi, T., Y. Fujinawa, M. Ukawa, and L. Bibot, Microearthquakes along the Back Arc Spreading System in the Bismarck Sea, Geo-Marine Letts., 6, 235-240,1987.

Engeln, J., and S. Stein, Tectonics of the Easter plate, Earth. Planet. Sci. Lett., 68, 259-270, 1984.

Engeln, J., S. Stein, J. Werner, and R. Gordon, Microplate and shear zone models for oceanic spreading center reorganizations, J. Geophys. Res., 93, 2839-2856, 1988.

Falvey, D. A., and T. Pritchard, Preliminary Paleomagnetic Results from Northern Papua New Guinea: Evidence for Large Microplate Rotations, Trans. Circum.-Pac. Counc. Energy Miner. Resour., 3, 593-600, 1985.

Hamburger, M., and B. Isacks, Diffuse back-arc deformation in the southwestern Pacific, Nature, 332, 599-604, 1988.

Hamilton, W., Tectonics of the Indonesian Region, U.S.G.S. Prof. Pap., 1078, 345 pp., U. S. Printing Office, Washington D. C., 1979.

Hey, R., A new class of pseudofaults and their bearing on plate tectonics: a propagating rift model, Earth Planet. Sci. Lett., 37, 321-325, 1977.

Hey, R., G. Johnson, and A. Lowrie, Recent Tectonic Evolution of the Galapagos Area and Plate Motions in the East Pacific, Geol. Soc. Am. Bull., 88, 1385-1403, 1977.

Hey, R., F. Duennebier, and W. Morgan, Propagating rifts on mid-ocean ridges, J. Geophys. Res., 85, 3647-3658, 1980.

Hey, R., and D. Wilson, Propagating Rift Explanation for Tectonic Evolution of the Northeast Pacific -- the Pseudo-Movie, Earth. Planet. Sci. Lett., 58, 167-188, 1982.

Hey, R., D. Naar, M. Kleinrock, W. Phipps-Morgan, E. Morales, and J. Schilling, Microplate Tectonics along a Superfast Seafloor Spreading System near Easter Island, Nature, 317, 320-325, 1985.

Hey, R., M. Kleinrock, S. Miller, T. Atwater, and R. Searle, Sea Beam/Deep Tow Investigation of an Active Oceanic Propagating Rift System Galapagos 95.5 W, J. Geophys. Res., 91, 3369-3394, 1986.

Hey, R., J. Sinton, and F. Duennebier, Propagating rifts and spreading centers, in Winterer, E., Hussong, D., and Decker, R., eds., The Eastern Pacific Ocean and Hawaii: Boulder, Colorado, Geological Society of America, The Geology of North America, v. N., Chap. 15, in press, 1988.

Hill, P., R. Reid, and J. Buleka, Marine geophysical survey of the west Woodlark Basin, M. V. 'Tapini', 1984-Cruise Report, BMR Record 1984/32, 1984.

Hobbs, B., W. Means, and P. Williams, An Outline of Structural Geology, 571 pp., John Wiley & Sons, New York, 1976.

Johnson, R., Geotectonics and volcanism in Papua New Guinea: a of the late Cainozoic, BMR J. Geol. & Geophys., 4, 181-207, 1979.

Johnson, R., J. Mutter, and R. Arculus, Origin of the Willaumez-Manus Rise, Papua New Guinea, Earth Planet. Sci. Lett., 44, 247-260, 1979.

Johnson, T., and P. Molnar, Focal Mechanisms and Plate Tectonics of the Southwest Pacific, J. Geophys. Res., 77, 5000-5032, 1972.

Kleinrock, M., Detailed Structural Studies of the Propagator System Near 95.5°W Along the Galapagos Spreading Axis, Ph. D. dissertation, 301pp., University of California at San Diego, 1988.

Kent, D., and F. Gradstein, A Jurassic to Recent chronology; in Vogt, P.,and B. Tucholke, eds., The Geology of North America, Volume M3, The Western North Atlantic: Geological Society of America, Chap. 3, 45-50, 1986.

Klitgord, K., S. Huestis, J., Mudie and R. Parker, An analysis of near-bottom magnetic anomalies: sea-floor spreading and the magnetized layer, Geophys. J. R. Astr. Soc., 43, 387-424, 1975.

Kroenke, L., Cenozoic tectonic development of the southwest Pacific, U.N. ESCAD, CCOP/SOPAC Technical Bull. 6, 122pp, CCOP/SOPAC, Suva, Fiji, 1984.

Lamb, S., Tectonic rotations about vertical axes during the last 4 Ma in part of the New Zealand plate-boundary zone, J. Struct. Geol., 10, 875-893, 1988.

Langmuir, C., J. Bender, and R. Batiza, Petrological and tectonic segmentation of the East Pacific Rise, 5° 30'-14° 30'N, Nature, 322, 422-429, 1986.

Lawver, L., J. Hawkins, and J. Sclater, Magnetic anomalies and crustal dilation in the Lau Basin, Earth. Planet. Sci. Lett., 33, 27-35, 1976.

Lawver, L. and J. Hawkins, Diffuse magnetic anomalies in marginal basins: their possible tectonic and petrologic significance, Tectonophysics, 45, 323-339, 1978.

Lindley, D., Early Cainozoic stratigraphy and structure of the Gazelle Peninsula east New Britain: an example of extensional tectonics in the New Britain arc-trench complex, Aust. J. Earth Sci., 35, 231-244, 1988.

Liu, L., Geochemistry and Petrology of Lavas From the Manus Basin Extensional Transform Zone and Manus Spreading Center: Implications for Source Compositions and Metasomatic Processes in Back-arc Basins, M. S. thesis, 94pp., University of Hawaii at Manoa, 1989.

Macdonald, K., Near-bottom magnetic anomalies, asymmetric spreading, oblique spreading and tectonics of the Mid-Atlantic Ridge near lat 37°N, Geol. Soc Amer. Bull., 88, 541-555, 1977.

Macdonald, K., and T. Holcombe, Inversion of magnetic anomalies and sea-floor spreading in the Cayman Trough, Earth Planet. Sci. Lett., 40, 407-414, 1978.

Mann, P., M. Hempton, D. Bradley, and K. Burke, Development of pull-apart basins, J. Geol., 91, 529-554, 1983.

McKenzie, D., The geometry of propagating rifts, Earth. Planet. Sci. Lett., 77, 176-186, 1986.

McKenzie, D., and J. Jackson, The relationship between strain rates, crustal thickening, palaeomagnetism, finite strain and fault movements within a deforming zone, Earth. Planet. Sci. Lett., 65, 182-202, 1983.

Miller, S., The validity of the geological interpretations of marine magnetic anomalies, Geophys. J. R. Astr. Soc., 50, 1-21, 1977.

Miller, S., K. Macdonald, and P. Lonsdale, Near-bottom magnetic profile across the Red Sea, Mar. Geophys Res., 7, 401-418, 1985.

Naar, D., and R. Hey, Fast rift propagation along the East Pacific Rise near Easter Island, J. Geophys. Res., 91, 3425-3438, 1986.

Parker, R., and S. Huestis, The inversion of magnetic anomalies in the presence of topography, J. Geophys. Res., 79, 1587-1593, 1974.

Pascal, G., Seismotectonics of the Papua New Guinea-Solomon Islands region, Tectonophysics, 57, 7-34, 1979.

Pigram, C., and H. Davies, Terranes and the accretion history of the New Guinea orogen, BMR J. Aust. Geol. and Geophys., 10, 193-211, 1987.

Ramsay, J., Folding and Fracturing of Rocks, 568 pp., McGraw-Hill Book Co., New York, 1967.

Ripper, I., Some Earthquake Focal Mechanisms in the New Guinea/Solomon Islands Region, 1963-1968, BMR Geol. and Geophys. Rept 178, 120 pp., 1975.

Ripper, I., Some earthquake focal mechanisms in the New Guinea/Solomon Islands region, BMR Geol. and Geophys. Rept. 192, 1977.

Schilling, J., H. Sigurdsson, A. Davis, and R. Hey, Easter microplate evolution, Nature, 317, 325-331, 1985.

Schouten, H., K. D., Klitgord, and D. G. Gallo, Microplate kinematics of the second order, in prep.

Sinton, J., D. Wilson, D. Christie, R. Hey, and J. Delaney, Petrologic consequences of rift propagation on oceanic spreading ridges, Earth. Planet. Sci. Lett., 62, 193-207, 1983.

Sinton, J., L. Liu, and B. Taylor, Petrology, magmatic budget and tectonic setting of Manus back-arc basin lavas (abstract), EOS Trans. AGU, 67, 377, 1986.

Sylvester, A., Strike-Slip Faults, G. S. A. Bull., 100, 1666-1703, 1988.

Taylor, B., Bismarck Sea: Evolution of a Back-arc Basin, Geology, 7, 171-174, 1979.

Taylor, B., A geophysical survey of the Woodlark-Solomons region, in Marine Geology, Geophysics, and Geochemistry of the Woodlark Basin-Solomon Islands, edited by B. Taylor and N. Exon, pp. 25-48, Circum-Pacific Council for Energy and Mineral Resources Earth Sci. Series, 7, Houston, Texas, Circum-Pacific Council for Energy and Mineral Resources, 1987.

Taylor, B., K. Crook, J. Sinton, and the Shipboard Party of Moana Wave, 8517 and 18, Fast spreading and sulfide deposition in Manus back-arc basin (abstract), A.A.P.G. Bull., 70, 936-937, 1986.

Taylor, B., R. Mallonee, K. Crook, and J. Sinton, The Manus Microplate (abstract), Eos Trans. AGU, 68, 1476, 1987.

Uyeda, S., Facts, ideas and open problems on trench-arc-backarc systems, in The Origin of Arcs, edited by F. -C. Wezel, pp. 435-460, Elsevier, Tokyo, 1986.

Weissel, J. K., Magnetic lineations in marginal basins of the western Pacific, Trans. R. Soc. Lond. A, 300, 223-247, 1981.

Weissel, J., B. Taylor, and G. Karner, The opening of the Woodlark Basin, subduction of the Woodlark spreading system, and the evolution of Northern Melanesia since mid-Pliocene time, Tectonophysics, 87, 253-277, 1982.

Wilson, D., and R. Hey, The Galapagos axial magnetic anomaly: Evidence for the Emperor event within the Brunhes and for a two-layer magnetic source, Geophys. Res. Lett., 8, 1051-1054, 1981.